

**KRAS Mutants Confer Platinum Resistance by Regulating ALKBH5
Post-translational Modifications in Lung Cancer**

Fang Yu^{1,2}, Shikan Zheng³, Chunjie Yu^{1,2}, Sanhui Gao^{1,2}, Zuqi, Shen^{1,2}, Rukiye Nar^{1,2},
Zhexin Liu^{1,2}, Shuang Huang⁵, Lizi Wu⁶, Tongjun Gu^{3,4}, and Zhijian Qian^{1,2*}

¹Department of Medicine, UF Health Cancer Center, University of Florida,
Gainesville, Florida, USA.

²Department of Biochemistry and Molecular Biology, University of Florida,
Gainesville, Florida, USA.

³Versiti Blood Research Institute, 8727 W Watertown Plank Rd, Milwaukee,
Wisconsin, USA.

⁴Department of Biostatistics, University of Florida, Gainesville, Florida, USA.

⁵Department of Anatomy & Cell Biology, University of Florida, Florida, USA.

⁶Department of Molecular Genetics and Microbiology, UF Health Cancer Center, UF
Genetic Institute, University of Florida, Florida, USA.

*Correspondence:

Zhijian.Qian@medicine.ufl.edu

Abstract

Constitutively active mutations of *KRAS* are prevalent in non-small cell lung cancer (NSCLC). However, the relationship between these mutations and resistance to platinum-based chemotherapy and the underlying mechanisms remain elusive. In this study, we demonstrated that *KRAS* mutants confer resistance to platinum in NSCLC. Mechanistically, *KRAS* mutants mediate platinum resistance in NSCLC cells by activating ERK/JNK signaling, which inhibits ALKBH5 m⁶A demethylase activity by regulating post-translational modifications (PTMs) of ALKBH5. Consequently, the *KRAS* mutant leads to a global increase in m⁶A methylation of mRNAs, particularly *DDB2* and *XPC*, which are essential for nucleotide excision repair. This methylation stabilized the mRNA of these two genes, thus enhancing NSCLC cells' capability to repair platinum-induced DNA damage and avoid apoptosis, thereby contributing to drug resistance. Furthermore, blocking *KRAS*-mutant-induced m⁶A methylation, either by overexpressing a SUMOylation-deficient mutant of ALKBH5, or by inhibiting METTL3 pharmacologically, significantly sensitizes *KRAS*-mutant NSCLC cells to platinum drugs in vitro and in vivo. Collectively, our study uncovers a mechanism that mediates *KRAS* mutant-induced chemoresistance in NSCLC cells by activating DNA repair through the modulation of the ERK/JNK/ALKBH5 PTMs-induced m⁶A modification in DNA damage repair-related genes.

Introduction

NSCLC is a frequently diagnosed malignancy and a leading cause of cancer-related deaths worldwide (1). Even when patients with NSCLC receive a combination of surgery and chemotherapy, the survival rate remains low due to cancer cells metastasis, invasion and drug resistance (2). Consequently, there is an urgent need to identify effective targets for inhibiting drug resistance in NSCLC.

Mutations in *KRAS* have been detected in up to 25% of NSCLC, which accounts for 85% of all lung cancer cases (3, 4). Although *KRAS* has been recognized as one of the most frequently mutated oncogenes in human malignancies since 1969, the lack of druggable pockets on *KRAS* protein surface, has resulted in only two FDA-approved drug until now (5, 6). However, these two FDA-approved *KRAS* inhibitors only specifically targets a particular *KRAS* mutation (*KRAS* G12C) (6, 7). Currently, platinum-based analogs like cisplatin and carboplatin are still commonly used for patients with *KRAS*-mutant NSCLC. Nonetheless, effectiveness of chemotherapy in *KRAS*-mutant NSCLC patients has been limited, failing to produce a lasting response (1, 8). Reports have indicated that *KRAS*-mutant NSCLC patients responded less favorably to cytotoxic therapy compared to patients with wild-type *EGFR* and *KRAS* genes (9-11). However, the question of whether and how *KRAS* mutations confer NSCLC platinum resistance remains unresolved.

Despite more than 170 chemical modifications on RNAs have been identified to date,

*N*⁶-methyladenosine (m⁶A) methylation remains the most abundant internal modification on eukaryotic messenger RNA (mRNA) (12). m⁶A methylation can be dynamically regulated by m⁶A writers, METTL3 and METTL14 as well as m⁶A erasers FTO and ALKBH5 (13-18). This reversible m⁶A methylation constitutes a new layer of post-transcriptional regulation of gene expression. m⁶A plays a pivotal role in governing almost all aspects of RNA metabolism, encompassing splicing, localization, translation, and stability, by recruiting a group of proteins termed as m⁶A readers. Although numerous studies have suggested that m⁶A methylation play crucial roles in the occurrence and development of various cancer types including NSCLC, the role of m⁶A methylation in chemoresistance in *KRAS*-mutant NSCLC remains elusive (19-21).

In this study, we investigated the role of *KRAS* constitutively active mutations in conferring platinum resistance in NSCLC. We demonstrated that *KRAS* mutants induce chemoresistance in NSCLC by amplifying EKR/JNK signaling-mediated ALKBH5 PTMs, including phosphorylation and SUMOylation. ALKBH5 PTMs lead to inhibition of ALKBH5 demethylase activity, resulting in an upregulation of m⁶A methylation within over a hundred of transcripts with alteration of expression. Among these transcripts, DDB2 and XPC that play an essential role in nucleotide excision (22, 23) are significantly upregulated as a consequence of an increase in m⁶A methylation in these transcripts. Notably, blocking the *KRAS* mutation-induced m⁶A increase in the DDB2 and XPC transcripts by METTL3 inhibition significantly sensitizes

NSCLC cells to platinum treatment, both in vitro and in vivo. This discovery provides a promising new avenue for the treatment of KRAS-mutant NSCLC. Collectively, our results illustrate how mRNA m⁶A modification adds an additional layer of complexity in mediating KRAS mutation-induced platinum resistance in NSCLC by regulating the expression of genes involved in DNA damage response. This study also represents the instance of a mutant *KRAS* oncogene hijacking the ALKBH5-PTMs/m⁶A methylation-mediated DNA damage response pathway to confer resistance to cytotoxic drugs in lung cancer cells.

Results

KRAS constitutively active mutations are associated with NSCLC platinum resistance

Despite the widespread occurrence of KRAS constitutively active mutations in lung cancers (24-26), the association between these mutations and platinum resistance in NSCLC has not been fully investigated. KRAS G12C (41%), KRAS G12V (22%) and KRAS G12D (12%) and KRAS G12A (9.3%) represent the most commonly observed mutations in KRAS within lung cancers (7, 27). We first established BEAS-2B cells derived from normal bronchial epithelium, stably expressing vector, KRAS constitutively active form (KRAS G12V), or a KRAS enzymatic mutant (KRAS S17N), and treated these cells with either DMSO or cisplatin. As shown in Figure 1A, the overexpression of constitutively active KRAS (KRAS G12V) but not KRAS enzymatic mutant (KRAS S17N) led to an increase in phosphorylated ERK and JNK protein levels in BEAS-2B cells. Notably, cisplatin treatment activates ERK/JNK signaling, and this activation can be further enhanced by the overexpression of KRAS G12V (Figure 1A). Meanwhile, cisplatin exposure significantly induced DNA damage in BEAS-2B cells, as evidenced by an increased expression of phosphorylated γ H₂AX, a sensitive marker of DNA damage (Figure 1A). Strikingly, KRAS-G12V significantly bolstered the resistance of BEAS-2B cells to cisplatin-induced DNA damage (Figure 1A). Next, we treated KRAS-wild-type NSCLC cells, including NCI-H522 and NCI-H292, KRAS G12C-mutant NSCLC cells, such as NCI-H23 and NCI-H2122, and KRAS G12A-mutant NSCLC cells, such as NCI-H1573 and

NCI-H2009, with either DMSO or cisplatin. Consistently, ERK/JNK signaling was more significantly activated, resulting in lower DNA damage in response to the chemotherapeutic drug in KRAS-mutant NSCLC cell lines, including NCI-H23, NCI-H2122, NCI-H1573, and NCI-H2009 as compared to KRAS wild-type lung cancer cell lines such as NCI-H522 and NCI-H292 (Figure 1B). Precise single-cell DNA damage analysis using the Alkaline Comet Assay revealed that KRAS wild-type NSCLC cells exhibit greater sensitivity to cisplatin-induced DNA damage compared to KRAS mutant lung cancer cells (Figure 1C and Supplemental Figure 1A). Additionally, cisplatin treatment markedly induced apoptosis in NCI-H522, whereas it had marginal effect on apoptosis of NCI-H23 cells (Figure 1D and Supplemental Figure 1B). We next examined colony forming ability of these cells. As shown in Figure 1E and Supplemental Figure 1C, NCI-H522 (KRAS wild-type) gave rise to fewer colonies than NCI-H23 (KRAS G12C) when the cells were treated with cisplatin. Collectively, these results suggest a positive correlation between KRAS constitutively active mutations and platinum resistance in NSCLC cells.

KRAS constitutively active mutations confer NSCLC platinum resistance

To rigorously investigate whether KRAS mutations confer platinum resistance in lung cancer cells, we adopted two approaches: overexpressing a constitutively active KRAS mutant in NCI-H522 (KRAS wild-type) and knocking down KRAS in NCI-H23 (KRAS G12C) cells. KRAS G12V overexpression markedly inhibited cisplatin-induced DNA damage and cell apoptosis in NCI-H522 cells (Figure 1, F and

G, and Supplemental Figure 1D). Conversely, KRAS knockdown (KD) greatly enhanced cisplatin-induced DNA damage and cell apoptosis in NCI-H23 cells (Figure 1, H and I, and Supplemental Figure 1, E and F). Except for the platinum-based drugs, paclitaxel (PTX) is also a frequently used chemotherapeutic drug in lung cancer treatment (28-31). Therefore, we next examined whether KRAS mutants induce paclitaxel resistance in lung cancer cells. As shown in Figure 1J-1O and Supplemental Figure 1G, KRAS-mutant NSCLC cells including H23 and H1573 and KRAS-wildtype NSCLCs including H522 and H292 are responsive to paclitaxel treatment while *KRAS* KD did not increase the sensitivity of H23 and H1573 NSCLC cells to paclitaxel treatment. However, we also observed that ERK/JNK signaling is highly activated in KRAS-mutant cells, exhibiting lower levels of DNA damage compared to KRAS wild-type cells when treated with other DNA damage reagents, such as Doxorubicin and Etoposide (Supplemental Figure 2, A and B). Taken together, these results provide compelling evidence that KRAS constitutively active mutations specifically confer platinum resistance, as well as other DNA damage inducers, but not paclitaxel in NSCLC cells.

KRAS-mutant-induced NSCLC platinum resistance is not mediated by ABC transporters

ATP-binding cassette (ABC) transporters are the largest and oldest membrane proteins in humans, which pump out various toxic compounds from the cells. The major cause of multidrug resistance (MDR) and chemotherapeutic failure is believed to be the

efflux of toxic drugs mediated by ABC transporters (32-34). Therefore, we next examined whether KRAS mutants-mediated platinum resistance is possibly mediated by ABC transporters. As shown in Supplemental Figure 2C-2E, the expression of ABC transporters including ABCB1, ABCG2, and ABCC1 are comparable in KRAS-wild-type and mutant NSCLC cells. Additionally, KRAS KD did not affect the expression of ABC transporters in KRAS-mutant lung cancer cells (Supplemental Figure 2F-2H). Together, these data suggest that KRAS-mutant-mediated NSCLC platinum resistance is not attributed to the dysregulation of ABC transporters.

The KRAS mutant regulates global mRNA m⁶A methylation via controlling ALKBH5 phosphorylation and SUMOylation

Our previously published study demonstrated that mammalian cells activate the ERK/JNK signaling to induce m⁶A methylation in DNA repair-related genes. This process safeguards the genomic stability by regulating ALKBH5 PTMs in response to oxidative stress (35). The ERK/JNK signaling pathway can be activated by ROS stress and oncogenes such as *KRAS* (24, 36-38). To examine whether the KRAS mutant regulates PTMs of ALKBH5, we established BEAS-2B cells, stably expressing vector, constitutively active KRAS mutant (KRAS G12V), and KRAS enzymatic mutant (KRAS S17N). Denaturing immunoprecipitation (IP) analysis of ALKBH5 revealed that expression of constitutively active KRAS significantly induced endogenous ALKBH5 phosphorylation and SUMOylation (Figure 2A and Supplemental Figure 3A). Consistently, inhibition of KRAS G12C by Sotorasib, or

ERK by PD0325901, significantly reduced both phosphorylation and SUMOylation of ALKBH5 in NCI-H23 cells. These findings suggest that ALKBH5 PTMs including phosphorylation and SUMOylation are driven by KRAS/ERK signaling (Supplemental Figure 3, B and C). In addition, both ALKBH5 phosphorylation-deficient mutant S325A and ALKBH5 SUMOylation-deficient mutant ALKBH5 K86R/K321R significantly reduced KRAS-G12V-induced ALKBH5 phosphorylation and SUMOylation (Figure 2, B and C and Supplemental Figure 3, D and E). These findings suggest that the constitutively active KRAS mutant induces ALKBH5 phosphorylation at serine 325 (S³²⁵), and SUMOylation at lysines 86 (K⁸⁶) and 321 (K³²¹). Given our previous study suggests that ALKBH5 phosphorylation triggers its SUMOylation, which in turn inhibits its m⁶A demethylase activity (35). Therefore, we checked whether the constitutively active KRAS mutant induces global mRNA m⁶A modification. Consistently, ectopic expression of KRAS G12V but not KRAS S17N markedly increased global mRNA m⁶A methylation in BEAS-2B cells (Figure 2D). To further determine the effect of the KRAS constitutively mutant on mRNA m⁶A methylation transcriptome-wide, we performed m⁶A-Seq analyses. We observed that KRAS G12V overexpression led to 1542 m⁶A peaks alterations in total among transcripts (Log2FC > 0.3, or Log2FC < -0.3, p < 0.05). Consistent with previous studies (13, 39, 40), the identified m⁶A peaks are located in sequences containing the canonical m⁶A methylation consensus motif RRACH (R = G or A; H = A, C, or U; where A is converted to m⁶A) (Supplemental Figure 3F). In line with the m⁶A level determined by dot-blot, m⁶A-Seq results

revealed that the majority of m⁶A peaks are upregulated upon KRAS G12V expression. Overall, 1259 peaks were upregulated and 283 peaks were downregulated (Figure 2, E and F and Supplemental Figure 3G). Additionally, Gene Ontology (GO) analysis of 1259 m⁶A peaks, which were significantly upregulated upon KRAS G12V overexpression showed that these peaks are enriched in the genes involved in pathways including RAS and MAPK signaling pathways, platinum drug resistance and nucleotide excision repair (Figure 2G). Platinum-based drugs serve as antitumor drugs mainly by facilitating cancer cells DNA damage through inducing cross-links formation between purine nucleotides (22, 41, 42). m⁶A-seq analysis suggests that the constitutively active KRAS mutant overexpression led to an m⁶A increase in the genes associated with nucleotide excision repair, suggesting an important role of nucleotide excision repair pathway in KRAS-mutant-mediated platinum resistance in lung cancer cells. Consistently, cisplatin-induced m⁶A increase in KRAS-mutant NCI-H23 cells was significantly higher as compared to KRAS wild-type NCI-H522 cells (Figure 2H). Meanwhile, inhibition of KRAS G12C or ERK effectively blocked cisplatin-induced m⁶A methylation in KRAS G12C-mutant NCI-H23 cells, suggesting that activation of KRAS/ERK signaling is responsible for the increased m⁶A methylation observed following cisplatin treatment (Supplemental Figure 3, H and I). Additionally, blocking mRNA m⁶A increase by expression of either ALKBH5 S325A, or ALKBH5 K86/321R significantly sensitized NCI-H23 cells to cisplatin-induced DNA damage (Figure 2, I and J). Conversely, overexpression of the ALKBH5 phosphorylation-mimic mutant ALKBH5 S325D, in KRAS wild-type H522 cells

significantly increased their resistance to cisplatin (Figure 2K). Collectively, these results suggest that the KRAS mutant regulates global mRNA m⁶A methylation by modulating ALKBH5 PTMs. Moreover, KRAS mutant-driven platinum resistance in NSCLC correlates with KRAS mutant-induced ALKBH5 PTMs.

Blocking ALKBH5 SUMOylation overcomes platinum resistance of NSCLC cells

Based on the aforementioned observations, we conducted a comparison of cisplatin-induced ALKBH5 PTMs between KRAS wild-type NCI-H522 and KRAS-mutant NCI-H23 cells. Notably, phosphorylation of ERK and JNK, as well as phosphorylation and SUMOylation of ALKBH5 were more significantly induced by cisplatin in NCI-H23 cells as compared to NCI-H522 cells (Figure 2L and Supplemental Figure 3J). In contrast, the levels of cisplatin-induced γ H2A.X in NCI-H522 cells were considerably higher than those in NCI-H23 cells (Supplemental Figure 3J). These results indicate that the KRAS mutant promotes chemoresistance in lung cancer cells, a phenomenon correlated with the upregulation of ERK/JNK signaling as well as increased ALKBH5 phosphorylation and SUMOylation. To further confirm that the KRAS mutant confers drug resistance via ALKBH5 SUMOylation in NSCLC cells, we inhibited ALKBH5 SUMOylation in both NCI-H522 and NCI-H23 cells by knocking down SUMO E2 UBC9. The results showed that KRAS-mutant NCI-H23 cells are more sensitive to UBC9 depletion as compared to KRAS-wild-type NCI-H522 cells and inhibition of ALKBH5 SUMOylation markedly enhances cisplatin-induced DNA damage and cell apoptosis

in KRAS-mutant cells (Figure 3A-3G). Together, these findings strongly suggest that cisplatin-induced ALKBH5 PTMs play important roles in drug resistance conferred by KRAS mutants.

Global transcriptomic and epitranscriptomic analyses identified nucleotide excision repair-related genes including DDB2 and XPC are key downstream target genes of the KRAS mutant

To further explore the molecular mechanism underlying KRAS-mutant-mediated platinum resistance in lung cancer, we performed RNA-seq analysis in control and KRAS G12V expressing NCI-H522 cells. As shown in Figure 4A, KRAS G12V led to significant alterations in gene expression, with 429 and 283 genes upregulated and downregulated, respectively ($\text{Log}_2\text{FC} > 0.3$, or $\text{Log}_2\text{FC} < -0.3$, $p < 0.05$). Gene Ontology (GO) analysis of those 712 differentially expressed genes induced by KRAS G12V revealed that the downstream target genes of the KRAS mutant are enriched in pathways involved in RAS and MAPK signaling pathways, platinum resistance, as well as pathways in cancer (Figure 4B). Additionally, Gene set enrichment analysis (GSEA) analyses revealed that the downstream target genes of the KRAS mutant are enriched in pathways involved in RAS signaling and DNA damage repair (Figure 4C-4D). By integrative analysis of RNA-seq and m⁶A-seq data, 105 genes were differentially expressed with an upregulation of m⁶A methylation level upon KRAS G12V expression. Gene Ontology (GO) analysis of these genes revealed that those genes are also enriched in the pathways involved in the activation of RAS and MAPK

signaling, as well as the platinum resistance (Figure 4, F and G). Among these genes, DDB2 and XPC stood out due to their important roles in multiple pathways that regulate the nucleotides excision repair and platinum resistance (22, 23) (Figure 4D, 4F and 4G). Notably, both the m⁶A methylation and expressions of DDB2 and XPC are significantly induced by KRAS G12V (Figure 4A, 4E, 4H and 4I). Consistent with the RNA-seq and m⁶A-seq results, both the transcription and mRNA m⁶A methylation level of DDB2 and XPC were significantly increased by KRAS G12V, as determined by qRT-PCR and the methylated RNA immunoprecipitation (MeRIP) followed by RT-PCR analyses, respectively. METTL3 KD, which blocks KRAS G12V-induced m⁶A methylation, significantly inhibited DDB2 and XPC expression (Figure 4J-4M), suggesting that the KRAS mutant regulates DDB2 and XPC mRNA expression in an m⁶A-dependent manner. Notably, KRAS G12V-induced upregulation of DDB2 and XPC was reversed by overexpression of a SUMOylation-deficient mutant ALKBH5 but not wild-type ALKBH5, suggesting that KRAS mutant regulates DDB2 and XPC expression through ALKBH5 SUMOylation (Supplemental Figure S4, A and B). We next investigated whether the KRAS-mutant drove platinum resistance, at least partially through the induction of DDB2 and XPC expression. As illustrated in Supplemental Figure 4, C and D, cisplatin treatment significantly induced the expression of DDB2 and XPC; and KRAS G12V further augmented cisplatin-induced expression of these genes in BEAS-2B cells (Supplemental Figure 4, C and D). In addition, cisplatin significantly induced expression of DDB2 and XPC in KRAS-wild-type NCI-H522 cells (Supplemental Figure 4, E and F). Notably, the

induction of expression of these genes was more significant in KRAS-mutant NCI-H23 cells compared to NCI-H522 cells (Supplemental Figure 4, E and F). These results suggest that enhanced nucleotide excision repair pathway with upregulation of DDB2 and XPC likely contributes to the resistance to chemotherapeutic drug in KRAS G12C-mutant NCI-H23. Collectively, these results indicate that the KRAS mutant induces chemoresistance possibly by facilitating the expression of nucleotide excision repair-related genes including DDB2 and XPC in an m⁶A-dependent manner in NSCLC cells.

Cisplatin/KRAS-induced m⁶A modification of *DDB2* and *XPC* lead to their mRNA stabilization

We next investigated the interplay between cisplatin-induced gene expression and the elevated m⁶A methylation levels of *DDB2* and *XPC*. As depicted in Figure 5, A and B, either expression of a SUMOylation-deficient mutant ALKBH5 or METTL3 KD by two specific shRNAs effectively blocked the cisplatin-induced m⁶A methylation increase of *DDB2* and *XPC*, leading to a downregulation of both genes in both NCI-H522 and NCI-H23 cells (Figure 5, C and D). Increased m⁶A methylation levels of *DDB2* and *XPC* in KRAS-mutant NCI-H23 resulted in the prolonged half-lives of *DDB2* and *XPC* mRNA compared to KRAS wild-type NCI-H522 cells. Cisplatin treatment significantly enhanced the stability of *DDB2* and *XPC* mRNA in KRAS-mutant NCI-H23 cells compared to KRAS wild-type NCI-H522 cells. Notably, the prolonged half-lives of *DDB2* and *XPC* mRNA induced by cisplatin in NCI-H522

and NCI-H23 cells were entirely reversed by expression of the SUMOylation-deficient ALKBH5 or by METTL3 KD (Figure 5E-5H). Similarly, either pharmacological inhibition of KRAS G12C or ERK completely reversed the prolonged mRNA half-lives of *DDB2* and *XPC* in KRAS G12C harboring H23 cells (Supplemental Figure 4G-4J). Thus, these results suggest that cisplatin-induced m⁶A methylation of *DDB2* and *XPC* leads to stabilization of their mRNA, which can be further augmented by the KRAS mutant in NSCLC cells.

KRAS mutations confer platinum resistance in NSCLC cells by modulating DDB2- and XPC-mediated nucleotide excision repair

Next, we aimed to uncover the mechanism underlying KRAS/ERK/ALKBH5 PTMs/DDB2&XPC signaling axis-mediated platinum resistance in NSCLC cells. Given that both DDB2 and XPC are key components of nucleotide excision repair (NER) machinery, we sought to determine whether the NER pathway is involved in KRAS mutation-driven platinum resistance in lung cancer. Consistent with previous studies (23, 43), knockdown of either *DDB2*, or *XPC* significantly reduced NER activity in NCI-H23 cells (Supplemental Figure 5A-5D). Notably, NER activity was significantly higher in *KRAS*-mutant NSCLC cells compared to *KRAS* wild-type lung cancer cells (Supplemental Figure 5, E and F), suggesting a positive correlation between *KRAS* mutations and NER activity in NSCLC cells. Additionally, KRAS G12V overexpression significantly enhanced NER activity in *KRAS* wild-type H522 cells (Supplemental Figure 5, G and H). Conversely, NER activity in *KRAS*-mutant

H23 cells was significantly inhibited by KRAS knockdown (Supplemental Figure 5, I and J). Together, these data provide compelling evidence that *KRAS* mutations positively regulate NER activity in NSCLC cells. Moreover, as shown in Supplemental Figure 6A-6F, knockdown of either *DDB2* or *XPC* significantly sensitized *KRAS*-mutant H23 cells to cisplatin-induced DNA damage. Furthermore, *KRAS* G12V overexpression-induced H522 cisplatin resistance was completely blocked by knockdown of either *DDB2*, or *XPC* (Figure 5I-5L). Collectively, these results suggest that *DDB2* and *XPC* play key roles in *KRAS* mutation-driven platinum resistance in NSCLC cells and that *KRAS* mutations confer drug resistance by enhancing NER activity.

ALKBH5 SUMOylation serves as a direct functional mediator in *KRAS* mutations-driven platinum resistance in NSCLC cells

RNA m⁶A methylation is dynamically regulated by m⁶A writer, of which the major catalytic subunit is METTL3, and erasers, including ALKBH5 and FTO (13, 35). Therefore, we investigated whether *KRAS* mutation-driven platinum resistance involves the regulation of FTO or METTL3 expression. Interestingly, *KRAS* G12V overexpression did not affect the protein levels of FTO or its PTMs, including phosphorylation and SUMOylation (Supplemental Figure 7A). Similarly, cisplatin resistance of *KRAS*-mutant H23 cells could not be overcome by FTO overexpression (Supplemental Figure 7B). Consistently, neither the cisplatin-induced expression, nor the m⁶A methylation of *DDB2* and *XPC* was restored by FTO overexpression

(Supplemental Figure 7C-7F), suggesting that DDB2 and XPC, as functional mediators of KRAS mutations, are specific downstream targets of ALKBH5. Moreover, KRAS G12V overexpression significantly upregulated METTL3 expression (Supplemental Figure 7, G and H). However, both KRAS G12V- and cisplatin-induced METTL3 expression were completely reversed by overexpression of a SUMOylation-deficient mutant ALKBH5 (Supplemental Figure 7, H and I), indicating that KRAS mutations induce METTL3 expression by regulating ALKBH5 SUMOylation. Collectively, these findings suggest that KRAS mutants-driven platinum resistance in NSCLC cells is mediated directly through the regulations of ALKBH5 SUMOylation. Furthermore, DDB2 and XPC, identified as functional mediators of KRAS mutants, are specific downstream targets of ALKBH5.

The KRAS mutant confers NSCLC drug resistance by hijacking ALKBH5 PTMs-mediated DNA repair pathways in vivo

To further determine whether KRAS mutation confers NSCLC drug resistance through KRAS/ERK/JNK/ALKBH5 PTMs/m⁶A/DDB2&XPC/nucleotide excision repair signaling axis in vivo, we carried out xenograft experiments with NSCLC cells. As shown in Figure 6A-6C, KRAS-mutant-NCI-H23 cells were more resistant to cisplatin treatment compared to KRAS wild-type NCI-H522 in vivo. Notably, ectopic expression of SUMOylation-deficient mutant ALKBH5 (SD-ALKBH5) significantly sensitized NCI-H23 cells to cisplatin treatment in vivo. Consistent with previously published studies (44, 45), the toxic effect of cisplatin treatment was minimal in our

experimental settings, as evidenced by the stable mouse weights and unaltered xenograft growth (Supplemental Figure 7J). In addition, ERK/JNK signaling was significantly more activated, resulting in lower levels of DNA damage in *KRAS*-mutant NCI-H23 cells in the xenograft model with cisplatin treatment compared to *KRAS* wild-type NCI-H522 xenografts (Figure 6D). Expression of SUMOylation-deficient mutant ALKBH5 (SD-ALKBH5) substantially facilitated cisplatin-induced DNA damage in NCI-H23 xenografts (Figure 6D). Consistently, ALKBH5 PTMs, including phosphorylation and SUMOylation, are significantly more pronounced in response to cisplatin treatment in *KRAS*-mutant H23 cells compared to *KRAS* wild-type H522 cells in vivo (Figure 6D). Moreover, global mRNA m⁶A methylation levels were induced more significantly in NCI-H23 xenografts by cisplatin treatment as compared to NCI-H522 xenografts (Figure 6E). SUMOylation-deficient mutant ALKBH5 (SD-ALKBH5) overexpression completely blocked cisplatin-induced mRNA m⁶A methylation in NCI-H23 xenografts (Figure 6E). More importantly, cisplatin treatment significantly induced m⁶A methylation of *DDB2* and *XPC* in *KRAS* wild-type NCI-H522 xenografts (Figure 6F and 6G). The induction of m⁶A methylation levels of these genes were even more pronounced in *KRAS*-mutant NCI-H23 xenografts (Figure 6F and 6G). Importantly, the cisplatin-induced m⁶A methylation of *DDB2* and *XPC* genes in *KRAS*-mutant NCI-H23 xenografts were blocked by overexpression of the SUMOylation-deficient mutant ALKBH5 (SD-ALKBH5) (Figure 6F and 6G). Consistently, the expression levels of *DDB2* and *XPC* were higher in NCI-H23 xenografts than in NCI-H522

xenografts with cisplatin treatment (Figure 6H and 6I). Overexpression of SUMOylation-deficient mutant ALKBH5 (SD-ALKBH5) blocked cisplatin-induced upregulation of *DDB2* and *XPC* in NCI-H23 xenografts (Figure 6H and 6I). Collectively, these results indicate that the *KRAS* mutant promotes platinum resistance in NSCLC cells in vivo by hijacking ALKBH5 PTMs-mediated DNA repair pathways.

METTL3 inhibition sensitizes *KRAS*-mutant NSCLC cells to cisplatin in vivo

To investigate whether *METTL3* KD exerts a similar rescue phenotype as ectopic expression of SD-ALKBH5, we established stable lines of NCI-H522 and NCI-H23 cells expressing scramble control, or *METTL3* specific shRNAs. As shown in Supplemental Figure 8 A and B, *METTL3* was significantly knockdown by both specific shRNAs. *METTL3* KD exhibited greater sensitivity to cisplatin-induced DNA damage and cell apoptosis in *KRAS*-mutant NCI-H23 cells compared to *KRAS* wild-type NCI-H522 cells (Figure 7A and Supplemental Figure 8C-8E). To assess the potential therapeutic application of targeting *METTL3* in *KRAS*-mutant NSCLC cells, we employed a small molecule STM2457, which potently and selectively inhibits *METTL3* enzymatic activity in a recent study (46). Consistently, *METTL3* inhibition by STM2457 markedly inhibited global mRNA m⁶A methylation in *KRAS*-mutant NCI-H23 cells (Figure 7B). Similar to *METTL3* KD, *METTL3* inhibition significantly sensitized NCI-H23 cells to cisplatin-induced DNA damage (Figure 7, C and D). Notably, γ -H2AX levels were increased upon *METTL3* inhibition in NSCLC

cells. METTL3 inhibition reduced m⁶A methylation in nucleotide excision-related genes, such as DDB2 and XPC, resulting in their mRNA decay and subsequent suppression of nucleotide excision repair activity. Additionally, METTL3 inhibition significantly enhanced the cisplatin-mediated suppression of the colony-forming ability of KRAS-mutant NCI-H23 cells (Figure 7E and Supplemental Figure 8F), and it markedly increased the sensitivity of NCI-H23 cells to cisplatin treatment in vivo (Figure 7F-7H). Meanwhile, in vivo METTL3 inhibition using STM2457 demonstrated minimal toxicity. Over a 40-day monitoring period, STM2457 injection didn't cause acute mortality or significant body weight loss in mice, nor did it visibly affect the morphology of major organs. Collectively, these results suggest that METTL3 is a promising and safe target for sensitizing *KRAS*-mutant NSCLC to cisplatin treatment.

KRAS mutants confer NSCLC drug resistance in primary lung cancer cells from patients

To further determine whether the aforementioned observations also exist in the primary lung cancer cells from patients, we collected three pairs of platinum-based chemotherapeutic primary lung adenocarcinoma tissues, both *KRAS* wild-type and mutant, from patients at UF Shands Hospital. As shown in Figure 8A, the ERK/JNK signaling is more significantly activated, resulting in lower levels of DNA damage in *KRAS*-mutant lung cancer cells compared to *KRAS* wild-type lung cancer cells from patients. Consistently, ALKBH5 PTMs, including phosphorylation and SUMOylation,

are much more abundant in *KRAS*-mutant primary lung cancer cells compared to *KRAS* wild-type cells (Figure 8A, right panel). Moreover, RT-qPCR analyses showed that both *DDB2* and *XPC* gene were expressed at much higher level in primary *KRAS*-mutant lung cancer cells compared to primary *KRAS* wild-type lung cancer cells (Figure 8B and 8C). In addition, the m⁶A methylation levels of *DDB2* and *XPC* transcripts were also higher in primary *KRAS*- mutant lung cancer cells compared to primary *KRAS* wild-type lung cancer cells (Figure 8D-8E). These findings suggest that the identified *KRAS*/*ERK*/*JNK*/*ALKBH5* PTMs/m⁶A/*DDB2*&*XPC*/nucleotide excision repair signaling axis is also active in primary lung cancer cells from patients. *KRAS* mutants confer platinum resistance at least partially through the post-transcriptional regulation of *DDB2* and *XPC* in an m⁶A-dependent manner, thereby facilitating the nucleotide excision of the cross-linked purine nucleotides induced by platinum-based chemotherapy drugs.

Discussion

Despite numerous therapeutic strategies have been developed for clinical lung cancer patient treatment, including surgical treatment, immunotherapy, radiation and chemotherapy, chemotherapy is still the critical component of the treatment regimen for the patients with NSCLC (6, 47-49). The efficacy of chemotherapy in *KRAS* mutant NSCLC patients is poor (50). The significance of *KRAS* as a prognosis marker in NSCLC is controversial (50). It was reported that *KRAS*-mutant NSCLC patients responded more poorly to cytotoxic therapy compared to *EGFR* wild-type/*KRAS* wild-type patients (9, 10). Platinum-based drugs exert its therapeutic effect by crosslinking purine bases on DNA, disrupting DNA repair processes, causing DNA damage and subsequently triggering cell apoptosis. Our studies demonstrated that *KRAS*-mutant NSCLC cells are more resistant to cisplatin treatment in vitro and in vivo. More importantly, we provide compelling evidence supporting that *KRAS* mutants confer NSCLC platinum resistance via inducing upregulation of m⁶A methylation of DNA repair genes, particularly *DDB2* and *XPC*. An increase of m⁶A methylation in *DDB2* and *XPC* transcripts leads to upregulation of *DDB2* and *XPC* expression through stabilizing their mRNAs. Consequently, the increased *DDB2* and *XPC* expression led to the accelerated excision of the cross-linked purine nucleotides, thereby conferring NSCLC platinum resistance. Upon cisplatin treatment, knockdown either *DDB2* or *XPC* gene increased DNA damage and induced apoptosis in *KRAS*-mutant NSCLC cells, thereby sensitizing these cells to cisplatin treatment. In addition, we showed that *KRAS*-mutants or *KRAS* KD do not affect the expression of

ABC transporters including ABCB1, ABCG2, and ABCC1 in NSCLC cells, ruling out the possibility that KRAS mutant-mediated NSCLC platinum resistance is a result of the dysregulation of ABC transporters. Moreover, we found that *KRAS*-mutant NSCLC cells are not resistant to paclitaxel (PTX), which is also a frequently used chemotherapeutic drug in lung cancer treatment (28-31). Thus, our data suggest that *KRAS*-mutant NSCLC cells are specifically resistant to cisplatin but not to paclitaxel, compared to *KRAS*-wild-type NSCLC cells. Additionally, DDB2 and XPC-mediated nucleotide excision repair pathway likely plays an important role in platinum-based chemoresistance. Notably, the KRAS mutant induces differential expression of over a hundred genes through upregulating m⁶A methylation of these genes, which are involved in RAS and MAPK signaling pathway and the platinum resistance. Thus, additional molecular pathways may also contribute to KRAS-mutant-mediated chemoresistance.

In this study, we uncovered a role of KRAS in regulating mRNA m⁶A methylation through regulating ALKBH5 PTMs in NSCLC cells. Although a previous study suggests that RAS/MAPK signaling regulates global mRNA m⁶A methylation through EKR-mediated phosphorylation of METTL3, thereby facilitating METTL3 protein stabilization by increasing USP5-mediated deubiquitination (51), our current study suggests that *KRAS*-mutants also regulates mRNA m⁶A methylation through inactivating ALKBH5 m⁶A demethylase activity by inducing ALKBH5 phosphorylation and SUMOylation.

Cisplatin treatment has been shown to induce oxidative stress, activating a DNA damage response through Reactive Oxygen Species (ROS) (52-57). Our previous study (35) demonstrated that ROS activate ERK/JNK signaling, leading to the phosphorylation of ALKBH5 at serine 325. This phosphorylation recruits the SUMO E2 enzyme UBC9, promoting ALKBH5 SUMOylation at lysine residues K86 and K321, which inhibits its m⁶A demethylase activity and upregulates genes involved in DNA damage repair.

In this study, we show that constitutively active *KRAS* mutations also induce ALKBH5 phosphorylation at serine 325, triggering its SUMOylation at the same lysine residues. This inactivates ALKBH5 and upregulates nucleotide excision repair-related genes, such as *DDB2* and *XPC* in an m⁶A-dependent manner, enhancing cisplatin resistance in NSCLC cells. Both ROS and *KRAS* mutations increase DNA repair capabilities by regulating ALKBH5 post-translational modifications (PTMs). Given that several studies (58, 59) suggest that *KRAS* overexpression also induces ROS production, *KRAS*-mediated ROS generation may also contribute to the *KRAS* mutations-driven platinum resistance in NSCLC cells. Notably, the ALKBH5 PTM sites induced by ROS and *KRAS* mutations are identical, suggesting a synergistic effect between ROS and *KRAS* mutations in driving platinum resistance, further reducing NSCL cell sensitivity to cisplatin. Our findings are supported by evidence: 1) *KRAS* G12C-induced ALKBH5 phosphorylation and SUMOylation were blocked by *KRAS* G12C or ERK inhibitors, confirming that RAS/ERK signaling is essential for

KRAS-driven ALKBH5 PTMs; (2) KRAS G12V overexpression induced SUMOylation of wild-type ALKBH5 but not the phosphorylation-deficient mutant S325D, indicating that SUMOylation depends on phosphorylation; and (3) ROS-triggered ALKBH5 phosphorylation, as shown in our previous study (35), leads to its SUMOylation via ERK/JNK signaling, and KRAS-induced PTMs occur at the same sites. However, the precise mechanism by which KRAS mutations induce ALKBH5 phosphorylation requires further investigation.

In conclusion, the interplay between oncogenic KRAS and ROS-mediated DNA damage response plays a critical role in the reduced sensitivity of KRAS-mutant NSCLC cells to platinum-based therapies. This underscores the importance of targeting the ERK/JNK/ALKBH5 PTM/NER signaling axis to overcome platinum resistance in these cells.

Despite being the most frequently mutated and activated oncogene in various cancers, targeting KRAS has posed a great therapeutic challenge over the past 50 years since its discovery. The development of small-molecule inhibitors relies on the availability of suitable binding pockets on the protein's surface. KRAS, however, has long been considered “undruggable” due to the absence of such binding pockets (5, 60). Therefore, although KRAS was identified as an oncogene as early as 1969, only two drugs specifically targeting KRAS G12C have received FDA approval (6). Despite this success, there remains a big challenge of combating the resistance that NSCLC

cells, xenografts, and patients have exhibited while treated with KRAS G12C inhibitors (6). Furthermore, published studies have revealed various KRAS mutations, including KRAS G12C, G12A, G12D, G12V, G12S, G12R, G12F, G13C, G13D, and Q61R in NSCLC cells (7, 61). Unfortunately, the current developed inhibitors can only target KRAS G12C. Additionally, many attempts have been made to target KRAS downstream pathways, specifically, the MAPK and PI3K-AKT pathways (62, 63). For example, the small molecules developed such as Selumetinib, which directly targets MEK, showed early promise, however further studies showed no statistically significant effects in *KRAS* mutant patients (63, 64). Therefore, treatment of *KRAS*-mutant lung cancer remains a challenge. Our current study suggests an alternative approach for the treatment. We found that blocking the cisplatin/*KRAS* mutation-induced m⁶A methylation through METTL3 inhibitor significantly enhances the sensitivity of *KRAS*-mutant NSCLC cells to cisplatin treatment, both in vitro and in vivo. This strategy allows us to combine METTL3 inhibitors with platinum-based drugs to treat the NSCLC cells, opening new avenues for the treatment of NSCLC patients.

In summary, our study has unraveled the intricate mechanisms through which KRAS mutations orchestrate the ERK/JNK signaling pathways, post-translational modifications of ALKBH5, and mRNA m⁶A modification to confer platinum resistance in NSCLC cells. We have shed light on molecular mechanisms by which KRAS constitutively active mutations elevate mRNA m⁶A methylation, thus adding

as a new layer of regulating ALKBH5 m⁶A demethylase activity, as well as gene regulation that fortifies DNA repair-related genes, shielding NSCLC cells from cisplatin-induced DNA damage and cell apoptosis. This ultimately facilitates chemoresistance in NSCLC (Figure 8F). Moreover, our research uncovered a mechanism by which KRAS mutants foster resistance to chemotherapy in NSCLC cells by hijacking ALKBH5 PTMs-mediated DNA damage response pathways (Figure 8F). Finally, we found that combining cisplatin with a METTL3 inhibitor significantly sensitizes *KRAS* mutant NSCLC cells to cisplatin exposure, offering a promising strategy for the treatment of NSCLC.

Methods

Sex as a biological variable. In all NSCLC NSGS mice xenograft studies, both male and female mice were used. Sex was not considered as a biological variable in the statistical analyses. The NSGS mice used for NSCLC xenograft studies were purchased from The Jackson laboratory.

Cell lines. Both the normal epithelial cells BEAS-2B, wild-type KRAS harboring NCI-H522, NCI-H2087, and KRAS mutant NSCLC cells including NCI-H23, NCI-H2122, NCI-H1573 and NCI-H2009 were kindly provided by Dr. Lizi Wu's lab at the Department of Molecular Genetics and Microbiology, UF Health Cancer Center, Gainesville, Florida. The BEAS-2B cells were cultured in the BEGM bronchial epithelial cell growth medium bulletkit (Lonza, Cat#CC-3170). For routine maintenance, all the NSCLC cells were cultured at 37 °C with 5% CO₂ in RPMI-1640 containing 10% FBS and 1% penicillin/streptomycin.

Plasmids and antibodies. The pCDH-Flag-KRAS G12V and pCDH-Flag-KRAS S17N were subcloned from plasmids kindly provided by Dr. Lizi Wu's lab at the Department of Molecular Genetics and Microbiology, UF Health Cancer Center, Gainesville, Florida. The pCDH-Strep-ALKBH5-HA expression plasmid was generated by cloning the corresponding coding sequence into pCDH-Strep vector. All the pCDH-Strep-HA-ALKBH5 K/R (lysine to arginine) or S/A (serine to alanine) mutants were derived from pCDH-Strep-HA-ALKBH5 by site-directed mutagenesis.

Information about antibodies used in this study were provided in Supplemental Table 1.

Drug treatment. For the lung cancer cell drug resistance analysis, the cells were treated with DMSO, or 20 μ M cisplatin for 24 hours. For the rescue experiment by METTL3 inhibition, the indicated cells were treated with 10 μ M STM2457 for 24 hours. For KRAS G12C inhibition, NCI-H23 cells were treated with 0.1 μ M sotorasib for 3h. For ERK inhibition, NCI-H23 cells were treated with 1 μ M PD0325901 for 3h.

Western blot analysis and Co-immunoprecipitation. The western blot and Co-immunoprecipitation analyses were performed according to standard protocols as described previously with minor changes (65), by using the antibodies as indicated. For examining SUMO-modified proteins, cells were lysed in denaturing buffer (50 mM Tris-HCl pH7.5, 150 mM NaCl, 4% SDS, 1mM EDTA, 8% glycerol, 50mM NaF, 1 mM DTT, 1mM PMSF and protease inhibitors) supplemented with 20 mM N-Ethylmaleimide (NEM) and heated at 90⁰C for 10 min. For the following immunoprecipitation assays, the lysates were further diluted to 0.1% SDS and immunoprecipitated with antibodies against target proteins at 4⁰C overnight. SUMO-modified proteins were then tested by Western blotting.

Alkaline Comet Assay. The alkaline comet analyses were performed with the cometAssay kit (R&D SYSTEMS, Cat# 4250-050-K) according to manufactory instructions with minor changes. Briefly, combine cells at 0.5 million per mL with

molten LMA agarose at a ratio of 1: 10 (v/v) and immediately pipette 80 μ L onto comet slice and place it at 4⁰C for 30 min in the dark. Immerse slice into 4⁰C lysis buffer for 1.5 hours. Next, immerse slice in alkaline unwinding solution (200 mM NaOH, 1 mM EDTA, pH>13) for 20 min at room temperature. Finally, Electrophoresis was performed in alkaline electrophoresis solution and the comet slices were stained with SYBR-Gold dye at room temperature for 30 min. The tail length was calculated by image J software.

shRNA knockdown and qRT-PCR. Knockdown of target genes by shRNAs was done as described previously (65). Scramble sequence and all the shRNAs against target genes were inserted into pLKO.1 vector. The sequences for shRNAs are listed in Supplemental Table S2. For qRT-PCR analysis, total RNA was extracted from various cells as indicated and reversely transcribed by using kits purchased from Thermo Fisher. The primer sequences used in the qRT-PCR are listed in Supplemental Table S2.

Cell apoptosis analysis by FACS. 0.5×10^6 of the indicated cells was treated with DMSO, or 20 μ M cisplatin for 24 hours. After that all the cells were collected and washed with ice-cold PBS and $1 \times$ AnnexinV binding buffer respectively. Then the cells were stained by 2.5 μ L anti-AnnexinV antibody and 1 μ M DAPI (Final concentration) in the dark and on ice for 30 min. After that the cells were subjected to flow cytometry analysis.

Lung cancer Xenograft studies. Animal experiments were performed according to animal protocols approved by animal core facility of University of Florida. Briefly, two million of lung adenocarcinoma cells were subcutaneously injected into two flanks of each NSGS mice. And 5 mg/kg cisplatin alone, or together with 30 mg/kg STM2457 was give i.p. every three days when tumor volume reaches $\sim 100 \text{ mm}^3$. Tumor volume and mice weight measurements were taken every 4 days and 7 days respectively. And, tumor volume was calculated according to formula: $[D \times (d^2)] / 2$ where D represents the large diameter of the tumor and d represents the small diameter of the tumor. Animals were individually monitored throughout the experiment.

Analysis of mRNA m⁶A methylation by dot-blot assay. mRNA m⁶A methylation was analyzed by dot-blot assays according to our published procedures with minor changes (13, 35). Briefly, total RNA was extracted using Trizol reagent (Thermo Fisher, Cat# 15596018), and mRNAs were separated using the dynabeads mRNA purification kit (Thermo Fisher, Cat# 61006). The mRNAs were denatured at 95 °C for 5 min, followed by chilling on ice directly. Next, 400 ng mRNAs was spotted to positively charged nylon (GE healthcare), air-dried for 5 min, and cross-linked using a 245 nm UV cross linker. The membranes were blocked in 5% non-fat milk plus 1% BSA in PBST for 2 hours and then incubated with anti- m⁶A antibodies at 4^oC overnight. After three times washing with PBST, the membranes were incubated with Alexa Fluor 680 Goat anti-rabbit IgG secondary antibodies at room temperature for 1

hour. Membranes were subsequently scanned using image studio. Methylene blue staining was used as a loading control to make sure equal amount of mRNAs was used for dot-blot analysis.

m⁶A RNA immunoprecipitation (MeRIP)-RT-qPCR Analysis. MeRIP analyses were performed according to the published paper (66). The primer sequences used in the qRT-PCR are listed in Table S1.

RNA stability assay for mRNA lifetime. All the indicated cells were treated with 5 µg per mL Actinomycin D and collected at indicated time points. The total RNA was extracted by Trizol reagent and subjected to RT-qPCR analysis. The primer sequences used in the qRT-PCR are listed in Supplemental Table 2.

m⁶A-Seq and RNA-Seq. Total RNAs were extracted from NCI-H522 cells stably expressing empty vector and KRAS G12V by Trizol reagent (Thermo Fisher, Cat# 15596018). 10 µg of total RNAs were fragmented with RNA fragmentation buffer (Thermo Fisher, Cat# AM8740). 1 µg of RNA fragments were kept for RNA-seq analysis. 9 µg of RNA fragments were used for IP enrichment by using anti-m⁶A antibody (Synaptic Systems, Cat# 202 003), namely for the m⁶A-seq analysis. Both the 1 µg of RNA fragments saved for the RNA-seq analysis and the m⁶A antibody enriched RNA fragments for m⁶A-seq analysis were rRNA depleted by using rRNA depletion kit (NEB, Cat# E6310L). Then the rRNA-depleted RNA fragments were

used to the sequence library construction by using the NEBNext® Ultra™ II Directional RNA Library Prep Kit for Illumina® (NEB, Cat# E7760L). Finally, purified cDNA libraries by using AMPure beads (Beckman coulter, Cat# A63881) were submitted to the next-generation sequencing service at the core facility of University of Florida for sequencing. All libraries were processed on a NovaSeq S4 2X150 platform (Illumina) with a paired-end 150-base pair read length and 50×10^6 reads per sample was required.

m⁶A-Seq and RNA-Seq data analysis. Bulk RNA-seq analysis: Bulk RNA-seq raw sequencing reads were aligned to the human genome, hg38, and sequencing quality and alignment rate was examined using Nextflow pipeline (nf-core/rnaseq 3.12)(67). Gene expression was quantified at the gene level using Salmon. RNA-seq libraries were then normalized using median of ratios method and genes were tested for differential expression between the empty vector and KRAS G12V overexpressed samples with DESeq2 v1.36(68). The Wald test was employed to identify differentially expressed genes. For visualization, pheatmap v1.0.12 was used for showing differential expression between samples. Gene Set Enrichment Test was performed using clusterProfiler v4.7.1(69). KEGG(70) and Reactome(71) databases were used in GSEA. To control the false positive rate, multiple testing correction was applied using the Benjamini-Hochberg method to adjust the P values obtained from both the differential expression analysis and GSEA. We set a significance threshold of adjusted P value at 0.05 to control the false discovery rate(72).

m⁶A-seq analysis

m⁶A-seq raw reads were trimmed using Trim Galore v0.6.10. FastQC v0.12 was used to examine the sequencing reads quality and low-quality reads were removed. Raw reads were aligned to human reference genome, hg38, Hisat2 v2.2.1(73). Peaks were

called using Macs2 v2.2.7.1(74). m⁶A-seq library were normalized to RNA-seq libraries using DiffBind v3.8.4(75). Differential analysis between empty vector and KRAS G12V overexpressed samples were performed using DESeq2 v1.38.3(68). For visualization, metagene plot was generated using Guitar v2.14.0(76). Motif analysis was performed using homer(77). To control the false positive rate, multiple testing correction was applied using the Benjamini-Hochberg method to adjust the P values obtained from both the differential expression analysis and GSEA. We set a significance threshold of adjusted P value at 0.05 to control the false discovery rate(72).

Statistical analysis. Results are presented as mean ± SD. Statistical analysis was calculated with 2-tailed Student's *t* test, or with ordinary 1-way ANOVA with Dunnett's multiple-comparison test using GraphPad Prism 9 software. The colony-forming assay, qRT-PCR, and cell culture experiments were done with 3 technical replicates and repeated at least 3 times. *P* values equal to or less than 0.05 were considered statistically significant. In all the results, "*" denotes $p < 0.05$, "***" denotes $p < 0.01$, "****" denotes $p < 0.001$, "*****" denotes $p < 0.0001$, and "ns" denotes no significant difference.

Study approval. All the animal studies are approved by the mouse core facility at the University of Florida.

Data availability. The raw and processed RNA-seq and m⁶A-Seq data have been deposited into NCBI Gene Expression Omnibus (GEO) database with accession number GSE268671. Values for all data points in graphs are reported in the Supporting data values file.

AUTHOR CONTRIBUTIONS

Z.Q. and F.Y. conceived the project. Z.Q. designed the research and supervised the experiments. F.Y., C.Y., S.G., N.R., conducted experiments and interpreted the data. Z.S., G.T., and S.Z., performed RNA-seq and m⁶A-seq data analysis. S.H and L.W. provided NSCLC cell lines and advice for the project. F.Y. and Z.Q. wrote the manuscript with inputs from all the other authors.

ACKNOWLEDGEMENTS

We thank members of Qian's laboratory for valuable discussion. This work was partially supported by National Institutes of Health (NIH) RO1 Grants R01 HL157539-01(Z.Q.), DK129489 (ZQ), CA259576-01(Z.Q.), R01CA266659 (Z.Q.). Z.Q. is Leukemia & Lymphoma Society (LLS) Scholars. We would also like to thank the Flow Cytometry Core and Sequencing Core at the University of Florida for their support.

DECLARATION OF INTERESTS

The authors have declared that no conflict of interest exists.

Address correspondence to: Zhijian Qian, Department of Medicine and Department of Biochemistry and Molecular Biology, UF Health Cancer Center, University of Florida, 2033 Mowry Road, Rm 257, Florida 32610, USA. Phone: 352-294-8984; Email: zhijian.qian@medicine.ufl.edu.

FIGURE LEGENDS

Figure 1. *KRAS* constitutively active mutation confers NSCLC platinum

resistance. (A) Western blots analysis showing protein levels as indicated in BEAS-2B cells. (B) Western blot analysis showing that the protein levels as indicated in *KRAS* wild-type or mutant NSCLC cells with or without cisplatin treatment. (C) Comet analysis for *KRAS* wild-type and mutant NSCLC cells with or without cisplatin treatment. (D) Cell apoptosis analyses for *KRAS* wild-type or mutant NSCLC cells with or without cisplatin treatment. (E) Colony-forming analyses for *KRAS* wild-type or mutant NSCLC cells with or without cisplatin treatment. (F) Annexin V staining analysis showing that overexpression of the *KRAS* mutant significantly inhibits cisplatin-induced cell apoptosis in NCI-H522 cells. (G) Western blot analysis showing that overexpression of the *KRAS* mutant significantly inhibits cisplatin-induced DNA damage in NCI-H522 cells. (H) Annexin V staining analysis showing that *KRAS* KD significantly facilitates cisplatin-induced cell apoptosis in NCI-H23 cells. (I) Western blot analysis showing that *KRAS* KD significantly promotes cisplatin-induced DNA

damage in NCI-H23 cells. **(J-M)** CCK8 analysis showing the effect of cisplatin and paclitaxel (PTX) treatment on the cell proliferation of *KRAS* wildtype and mutant NSCLC cells. **(N and O)** CCK8 analysis indicating the effect of *KRAS* KD on paclitaxel (PTX) sensitivity of *KRAS* mutant cells. In **C-F, H, and J-O**, data are presented as mean \pm SD, with ordinary 1-way ANOVA with Dunnett's multiple-comparison test used for **C-D, F, H, and J-O** and 2-tailed Student's *t* test for **E**. * $P < 0.05$, ** $P < 0.01$, *** $P < 0.001$, **** $P < 0.0001$.

Figure 2. The constitutively active KRAS mutant regulates global mRNA m⁶A methylation via controlling ALKBH5 phosphorylation and SUMOylation. **(A)** Denaturing IP analysis suggests overexpression of the constitutively active *KRAS* mutant significantly induces ALKBH5 phosphorylation and SUMOylation in BEAS-2B cells. **(B)** IP analysis suggesting the *KRAS*-mutant mediates ALKBH5 phosphorylation at serine residue 325. **(C)** Denaturing IP analysis suggests that overexpression of the constitutively active *KRAS* mutant induces ALKBH5 SUMOylation at lysine residues 86 and 321. **(D)** Dot-blot analysis suggests global mRNA m⁶A methylation could be induced by overexpression of the constitutively active *KRAS* mutant. **(E)** Heat map showing mRNA transcripts with significant m⁶A modification alterations upon *KRAS* G12V overexpression in NCI-H522 cells identified by m⁶A-seq analysis. **(F)** The frequency distribution of m⁶A peaks across the length of mRNA transcripts shown by metagene analysis in empty vector and *KRAS* G12V overexpressed NCI-H522 cells. **(G)** Gene ontology (GO) analysis of

genes, of which m⁶A methylation were significantly upregulated by KRAS G12V overexpression. (H) Dot blot analysis indicating global mRNA m⁶A methylation in *KRAS* wild-type and mutant NSCLC cells with or without cisplatin treatment. (I) Western blots analysis suggests that overexpression of the ALKBH5 phosphorylation-deficient mutant significantly sensitizes *KRAS* mutant harboring NCI-H23 cells to cisplatin-induced DNA damage. (J) Western blots analysis suggests that overexpression of the ALKBH5 SUMOylation-deficient mutant significantly sensitizes *KRAS* mutant harboring NCI-H23 cells to cisplatin-induced DNA damage. (K) Western blots analysis indicates that overexpression of the phosphorylation-mimic mutant ALKBH5 S325D significantly enhances the cisplatin sensitivity of *KRAS* wild-type H522 cells. (L) Denaturing IP analysis showing ALKBH5 phosphorylation and SUMOylation in *KRAS* wild-type and mutant NSCLC cells with or without cisplatin treatment.

Figure 3. Blocking ALKBH5 SUMOylation overcomes platinum resistance of NSCLC cells. (A) Western blot analysis showing the effect of ALKBH5 SUMOylation blocking by UBC9 KD on the cisplatin sensitivity of *KRAS* wild-type NCI-H522 cells. (B) Histograms showing the summary and statistical analysis of the grey value of western bands shown in Figure 3A. (C) Western blot analysis showing the effect of ALKBH5 SUMOylation blocking by UBC9 KD on the cisplatin sensitivity of *KRAS* mutant NCI-H23 cells. (D) Histograms showing the summary and statistical analysis of the grey value of western bands shown in Figure 3C. (E) Western blot analysis showing

the knockdown efficiency of UBC9 in both NCI-H522 and NCI-H23 cells. (F) Cell apoptosis analysis suggests that blocking ALKBH5 SUMOylation by *UBC9* KD significantly sensitizes *KRAS*-mutant NCI-H23 cells to cisplatin-induced cell apoptosis. (G) Histograms showing the summary and statistical analysis of the data shown in Figure 3F. In **B**, **D**, and **G**, data are presented as mean \pm SD, with ordinary 1-way ANOVA with Dunnett's multiple-comparison test used. * $P < 0.05$, ** $P < 0.01$, *** $P < 0.001$, **** $P < 0.0001$.

Figure 4. Global transcriptomic and epitranscriptomic analyses identified nucleotide excision repair-related genes including *DDB2* and *XPC* are key downstream target genes of the *KRAS* mutant. (A) Volcano figure showing the differentially expressed genes induced by *KRAS* G12V overexpression in NCI-H522 cells. (B) Gene ontology (GO) analysis of the differentially expressed genes induced by *KRAS* G12V overexpression. (C) GSEA plot showing enrichment of gene sets of DNA damage repair and *KRAS* signaling in *KRAS* G12V-overexpressed NCI-H522 cells. (D) Heatmap showing the increased genes list of DNA damage repair-related genes induced by *KRAS* G12V overexpression shown in Figure 4C. (E) Distribution of genes identified by m⁶A-seq with significant changes in both mRNA m⁶A methylation and overall expression induced by *KRAS* G12V overexpression. (F) The venn diagram shows the overlapped genes with both significant expression and m⁶A alterations upon *KRAS* G12V overexpression. (G) Gene ontology (GO) analysis of *KRAS* G12V

downstream target genes in an m⁶A-dependent manner, identified by integrative analysis of RNA-seq and m⁶A-seq data in NCI-H522 cells. (**H** and **I**) RNA-seq and m⁶A-seq peaks visualization of *DDB2* and *XPC* transcripts in empty vector- and KRAS G12V-overexpressed NCI-H522 cells. (**J** and **K**) RT-qPCR analysis suggests that KRAS G12V-overexpression-mediated upregulation of *DDB2* and *XPC* could be rescued by METTL3 KD. (**L** and **M**) MeRIP analyses suggest that KRAS G12V-overexpression-induced upregulation of m⁶A methylation levels of *DDB2* and *XPC* transcripts is blocked by METTL3 depletion. In **J-M**, data are presented as mean \pm SD, with ordinary 1-way ANOVA with Dunnett's multiple-comparison test used. **P* < 0.05, ***P* < 0.01, ****P* < 0.001, *****P* < 0.0001.

Figure 5. Cisplatin/KRAS-induced m⁶A modification of *DDB2* and *XPC* lead to their mRNA stabilization. (**A** and **B**) MeRIP analyses showing mRNA m⁶A levels of *DDB2* and *XPC* in the NSCLC cells as indicated. (**C** and **D**) RT-qPCR analysis for *DDB2* and *XPC* in the cell lines as indicated. (**E** and **H**) Analysis of mRNA half-lives of *DDB2*, and *XPC* in the NSCLC cells as indicated. (**I** and **J**) RT-qPCR analysis showing the KD efficiency of *DDB2* and *XPC* in NCI-H23 cells, respectively. (**K** and **L**) Western blot analyses suggest that either *DDB2*, or *XPC* KD significantly sensitizes KRAS G12V overexpressed NCI-H522 cells to cisplatin treatment. In **A-J**, data are presented as mean \pm SD, with ordinary 1-way ANOVA with Dunnett's multiple-comparison test used. **P* < 0.05, ***P* < 0.01, ****P* < 0.001, *****P* < 0.0001.

Figure 6. KRAS constitutively active mutation confers NSCLC drug resistance by hijacking AKBH5 PTMs-mediated DNA repair pathways in vivo. (A-C) Effects of cisplatin injection and overexpression of SUMOylation-deficient mutant ALKBH5 (SD-ALKBH5) on tumor growth of NCI-H522 and NCI-H23 xenograft mice. n=3 mice for each group and lung cancer cells as indicated were injected at two flanks of each mouse. (D) Denature IP analysis showing the ALKBH5 PTMs levels in the indicated lung cancer xenografts. Proteins were extracted from three tumors, each obtained from a different mouse, and then combined into a single mixture for the IP analysis. (E) Dot-blot analysis suggesting global mRNA m⁶A levels in the xenografts as indicated. RNAs were extracted from three tumors, each obtained from a different mouse, and then combined into a single mixture for the dot-blot analysis. (F and G) MeRIP analysis showing mRNA m⁶A levels of *DDB2* and *XPC* in the xenografts as indicated. (H and I) RT-qPCR analysis indicating transcription levels of *DDB2* and *XPC* in the xenografts as indicated. In B-C, and F-I, data are presented as mean ± SD, with ordinary 1-way ANOVA with Dunnett's multiple-comparison test used. **P* < 0.05, ***P* < 0.01, ****P* < 0.001, *****P* < 0.0001.

Figure 7. METTL3 inhibition sensitizes KRAS mutation harboring NSCLC cells to cisplatin in vivo. (A) Annexin V staining analysis for the NSCLC cells as indicated. (B) Dot-blot analysis showing the effect of METTL3 inhibition on global mRNA m⁶A

methylation levels in NCI-H23 cells. (C) Western blot analysis indicates that METTL3 inhibition by 10 uM STM2457 significantly sensitizes *KRAS* mutation harboring NCI-H23 cells to cisplatin-induced DNA damage. (D) Histograms showing the summary and statistical analysis of the grey value of western bands shown in Figure 7C. (E) Colony forming analysis for the NSCLC cells as indicated. (F-H) NSCLC xenograft experiments suggest that pharmacological inhibition of METTL3 markedly sensitizes *KRAS*-mutant NCI-H23 cells to cisplatin treatment in vivo. n=3 mice for each group and lung cancer cells as indicated were injected at two flanks of each mouse. In A, D-E, and G-H, data are presented as mean \pm SD, with ordinary 1-way ANOVA with Dunnett's multiple-comparison test used for D-E, and G-H and 2-tailed Student's *t* test for A. * $P < 0.05$, ** $P < 0.01$, *** $P < 0.001$, **** $P < 0.0001$.

Figure 8. *KRAS*/ERK/JNK/ALKBH5 PTMs/m⁶A/DDB2&XPC/nucleotide excision repair signaling axis occurs frequently among clinical lung cancer patients (A) Western blot analysis showing the protein levels as indicated in the indicated clinical platinum-based chemotherapeutic lung cancer samples. (B and C) RT-qPCR analysis showing the mRNA levels of *DDB2* and *XPC* in *KRAS* wild-type and mutant lung cancer patient samples. (D and E) MeRIP analysis showing the mRNA m⁶A levels of *DDB2* and *XPC* in *KRAS* wild-type and mutant lung cancer patient samples. (F) Working model of *KRAS*-mutant-mediated platinum resistance in NSCLC. In *KRAS* wild-type lung cancer cells, cisplatin treatment cause DNA damage

by inducing purine nucleotide crosslinking, ultimately triggering apoptosis. However, in *KRAS*-mutant lung cancer cells, *KRAS* mutations activate ERK/JNK signaling, leading to ALKBH5 phosphorylation and subsequent SUMOylation. This SUMOylation inhibits its m⁶A demethylase activity, leading to a global increase in mRNA m⁶A methylation, including on nucleotide excision repair-related genes such as *DDB2* and *XPC*. The stabilization of *DDB2* and *XPC* mRNA enhances nucleotide excision repair, allowing *KRAS* mutations to drive chemoresistance. In **B-E**, data are presented as mean \pm SD, with ordinary 1-way ANOVA with Dunnett's multiple-comparison test used for **D** and **E** and 2-tailed Student's *t* test for **B** and **C**. **P* < 0.05, ***P* < 0.01, ****P* < 0.001, *****P* < 0.0001.

Reference

1. Bray F, Ferlay J, Soerjomataram I, Siegel RL, Torre LA, and Jemal A. Global cancer statistics 2018: GLOBOCAN estimates of incidence and mortality worldwide for 36 cancers in 185 countries. *CA: a cancer journal for clinicians*. 2018;68(6):394-424.
2. Torre LA, Bray F, Siegel RL, Ferlay J, Lortet - Tieulent J, and Jemal A. Global cancer statistics, 2012. *CA: a cancer journal for clinicians*. 2015;65(2):87-108.
3. Molina JR, Yang P, Cassivi SD, Schild SE, and Adjei AA. *Mayo Clinic Proceedings*. Elsevier; 2008:584-94.
4. Román M, Baraibar I, López I, Nadal E, Rolfo C, Vicent S, et al. KRAS oncogene in non-small cell lung cancer: clinical perspectives on the treatment of an old target. *Molecular cancer*. 2018;17(1):33.
5. Yu F, and Qian Z. Mechanisms for regulation of RAS palmitoylation and plasma membrane trafficking in hematopoietic malignancies. *Journal of Clinical Investigation*. 2023;133(12):e171104.
6. Batrash F, Kutmah M, and Zhang J. The current landscape of using direct inhibitors to target KRASG12C-mutated NSCLC. *Experimental Hematology & Oncology*. 2023;12(1):93.
7. Parikh K, Banna G, Liu SV, Friedlaender A, Desai A, Subbiah V, et al. Drugging KRAS: current perspectives and state-of-art review. *Journal of Hematology & Oncology*. 2022;15(1):152.
8. Yang H, Liang SQ, Schmid RA, and Peng RW. New Horizons in KRAS-Mutant Lung Cancer: Dawn After Darkness. *Front Oncol*. 2019;9:953.
9. Metro G, Chiari R, Bennati C, Cenci M, Ricciuti B, Puma F, et al. Clinical outcome with platinum-based chemotherapy in patients with advanced nonsquamous EGFR wild-type non-small-cell lung cancer segregated according to KRAS mutation status. *Clin Lung Cancer*. 2014;15(1):86-92.
10. Hames ML, Chen H, Iams W, Aston J, Lovly CM, and Horn L. Correlation between KRAS mutation status and response to chemotherapy in patients with advanced non-small cell lung cancer. *Lung Cancer*. 2016;92:29-34.
11. Marabese M, Ganzinelli M, Garassino MC, Shepherd FA, Piva S, Caiola E, et al. KRAS mutations affect prognosis of non-small-cell lung cancer patients treated with first-line platinum containing chemotherapy. *Oncotarget*. 2015;6(32):34014-22.
12. Frye M, Harada BT, Behm M, and He C. RNA modifications modulate gene expression during development. *Science*. 2018;361(6409):1346-9.
13. Yu F, Zhu AC, Liu S, Gao B, Wang Y, Khudaverdyan N, et al. RBM33 is a unique m6A RNA-binding protein that regulates ALKBH5 demethylase activity and substrate selectivity. *Molecular Cell*. 2023.
14. Bokar JA, Rath-Shambaugh ME, Ludwiczak R, Narayan P, and Rottman F. Characterization and partial purification of mRNA N6-adenosine methyltransferase from HeLa cell nuclei. Internal mRNA methylation requires a multisubunit complex. *Journal of Biological Chemistry*. 1994;269(26):17697-704.
15. Bokar J, Shambaugh M, Polayes D, Matera A, and Rottman F. Purification and cDNA cloning of the AdoMet-binding subunit of the human mRNA (N6-adenosine)-methyltransferase. *Rna*. 1997;3(11):1233-47.
16. Liu J, Yue Y, Han D, Wang X, Fu Y, Zhang L, et al. A METTL3–METTL14 complex mediates mammalian nuclear RNA N 6-adenosine methylation. *Nature chemical biology*.

- 2014;10(2):93.
17. Jia G, Fu Y, Zhao X, Dai Q, Zheng G, Yang Y, et al. N6-methyladenosine in nuclear RNA is a major substrate of the obesity-associated FTO. *Nature chemical biology*. 2011;7(12):885.
 18. Zheng G, Dahl JA, Niu Y, Fedorcsak P, Huang C-M, Li CJ, et al. ALKBH5 is a mammalian RNA demethylase that impacts RNA metabolism and mouse fertility. *Molecular cell*. 2013;49(1):18-29.
 19. Jin D, Guo J, Wu Y, Yang L, Wang X, Du J, et al. m6A demethylase ALKBH5 inhibits tumor growth and metastasis by reducing YTHDFs-mediated YAP expression and inhibiting miR-107/LATS2-mediated YAP activity in NSCLC. *Molecular cancer*. 2020;19:1-24.
 20. Guo J, Wu Y, Du J, Yang L, Chen W, Gong K, et al. Deregulation of UBE2C-mediated autophagy repression aggravates NSCLC progression. *Oncogenesis*. 2018;7(6):1-16.
 21. Zhang D, Ning J, Okon I, Zheng X, Satyanarayana G, Song P, et al. LKB1 Loss Upregulates ALKBH5 and Contributes to Aggressive Phenotypes of KRAS Mutated Lung Cancer. 2020.
 22. Stefanou DT, Souliotis VL, Zakopoulou R, Lontos M, and Bamias A. DNA damage repair: predictor of platinum efficacy in ovarian cancer? *Biomedicines*. 2021;10(1):82.
 23. Ribeiro-Silva C, Sabatella M, Helfricht A, Martejn JA, Theil AF, Vermeulen W, et al. Ubiquitin and TFIIH-stimulated DDB2 dissociation drives DNA damage handover in nucleotide excision repair. *Nature communications*. 2020;11(1):4868.
 24. Pritchard AL, and Hayward NK. Molecular pathways: mitogen-activated protein kinase pathway mutations and drug resistance. *Clinical cancer research*. 2013;19(9):2301-9.
 25. Yang MH, Nickerson S, Kim ET, Liot C, Laurent G, Spang R, et al. Regulation of RAS oncogenicity by acetylation. *Proceedings of the National Academy of Sciences*. 2012;109(27):10843-8.
 26. San Tam IY, Chung LP, Suen WS, Wang E, Wong MC, Ho KK, et al. Distinct epidermal growth factor receptor and KRAS mutation patterns in non-small cell lung cancer patients with different tobacco exposure and clinicopathologic features. *Clinical Cancer Research*. 2006;12(5):1647-53.
 27. Garassino M, Marabese M, Rusconi P, Rulli E, Martelli O, Farina G, et al. Different types of K-Ras mutations could affect drug sensitivity and tumour behaviour in non-small-cell lung cancer. *Annals of oncology*. 2011;22(1):235-7.
 28. Li R, Moudgil T, Ross H, and Hu H-M. Apoptosis of non-small-cell lung cancer cell lines after paclitaxel treatment involves the BH3-only proapoptotic protein Bim. *Cell Death & Differentiation*. 2005;12(3):292-303.
 29. Fujishita T, Loda M, Turner RE, Gentler M, Kashii T, Breathnach OS, et al. Sensitivity of non-small-cell lung cancer cell lines established from patients treated with prolonged infusions of Paclitaxel. *Oncology*. 2003;64(4):399-406.
 30. Belani CP, Choy H, Bonomi P, Scott C, Travis P, Haluschak J, et al. Combined chemoradiotherapy regimens of paclitaxel and carboplatin for locally advanced non-small-cell lung cancer: A randomized phase II locally advanced multi-modality protocol. *Journal of clinical oncology*. 2005;23(25):5883-91.
 31. Pirker R, Krajnik G, Zöchbauer S, Malayeri R, Kneussl M, and Huber H. Paclitaxel/cisplatin in advanced non-small-cell lung cancer (NSCLC). *Annals of oncology*. 1995;6(8):833-5.
 32. Kathawala RJ, Gupta P, Ashby Jr CR, and Chen Z-S. The modulation of ABC transporter-mediated multidrug resistance in cancer: a review of the past decade. *Drug*

- resistance updates*. 2015;18:1-17.
33. Rees DC, Johnson E, and Lewinson O. ABC transporters: the power to change. *Nature reviews Molecular cell biology*. 2009;10(3):218-27.
 34. Wang JQ, Wu ZX, Yang Y, Teng QX, Li YD, Lei ZN, et al. ATP - binding cassette (ABC) transporters in cancer: A review of recent updates. *Journal of Evidence - Based Medicine*. 2021;14(3):232-56.
 35. Yu F, Wei J, Cui X, Yu C, Ni W, Bungert J, et al. Post-translational modification of RNA m6A demethylase ALKBH5 regulates ROS-induced DNA damage response. *Nucleic acids research*. 2021;49(10):5779-97.
 36. Benvenuti S, Sartore-Bianchi A, Di Nicolantonio F, Zanon C, Moroni M, Veronese S, et al. Oncogenic activation of the RAS/RAF signaling pathway impairs the response of metastatic colorectal cancers to anti-epidermal growth factor receptor antibody therapies. *Cancer research*. 2007;67(6):2643-8.
 37. Zeke A, Misheva M, Reményi A, and Bogoyevitch MA. JNK signaling: regulation and functions based on complex protein-protein partnerships. *Microbiol Mol Biol Rev*. 2016;80(3):793-835.
 38. Santarpia L, Lippman SM, and El-Naggar AK. Targeting the MAPK-RAS-RAF signaling pathway in cancer therapy. *Expert opinion on therapeutic targets*. 2012;16(1):103-19.
 39. Shen C, Sheng Y, Zhu AC, Robinson S, Jiang X, Dong L, et al. RNA demethylase ALKBH5 selectively promotes tumorigenesis and cancer stem cell self-renewal in acute myeloid leukemia. *Cell stem cell*. 2020;27(1):64-80. e9.
 40. Liu J, Gao M, He J, Wu K, Lin S, Jin L, et al. The RNA m6A reader YTHDC1 silences retrotransposons and guards ES cell identity. *Nature*. 2021;591(7849):322-6.
 41. Gumulec J, Balvan J, Sztalmachova M, Raudenska M, Dvorakova V, Knopfova L, et al. Cisplatin-resistant prostate cancer model: Differences in antioxidant system, apoptosis and cell cycle. *International Journal of Oncology*. 2014;44(3):923-33.
 42. Rocha CRR, Silva MM, Quinet A, Cabral-Neto JB, and Menck CFM. DNA repair pathways and cisplatin resistance: an intimate relationship. *Clinics*. 2018;73:e478s.
 43. Kusakabe M, Onishi Y, Tada H, Kurihara F, Kusao K, Furukawa M, et al. Mechanism and regulation of DNA damage recognition in nucleotide excision repair. *Genes and Environment*. 2019;41:1-6.
 44. Jin L, Chun J, Pan C, Li D, Lin R, Alesi GN, et al. MAST1 drives cisplatin resistance in human cancers by rewiring cRaf-independent MEK activation. *Cancer cell*. 2018;34(2):315-30. e7.
 45. Higgins B, Kolinsky K, Smith M, Beck G, Rashed M, Adames V, et al. Antitumor activity of erlotinib (OSI-774, Tarceva) alone or in combination in human non-small cell lung cancer tumor xenograft models. *Anti-cancer drugs*. 2004;15(5):503-12.
 46. Yankova E, Blackaby W, Albertella M, Rak J, De Braekeleer E, Tsagkogeorga G, et al. Small-molecule inhibition of METTL3 as a strategy against myeloid leukaemia. *Nature*. 2021;593(7860):597-601.
 47. Johnson DH, Schiller JH, and Bunn Jr PA. Recent clinical advances in lung cancer management. *Journal of clinical oncology*. 2014;32(10):973-82.
 48. Cagle PT, and Chirieac LR. Advances in treatment of lung cancer with targeted therapy. *Archives of pathology & laboratory medicine*. 2012;136(5):504-9.
 49. Zhao F, Shen D, Shang M, Yu H, Zuo X, Chen L, et al. Immunotherapy: A new target for cancer cure. *Oncology Reports*. 2023;49(5):1-14.

50. Ferrer I, Zugazagoitia J, Herbertz S, John W, Paz-Ares L, and Schmid-Bindert G. KRAS-Mutant non-small cell lung cancer: From biology to therapy. *Lung Cancer*. 2018;124:53-64.
51. Sun H-L, Zhu AC, Gao Y, Terajima H, Fei Q, Liu S, et al. Stabilization of ERK-phosphorylated METTL3 by USP5 increases m6A methylation. *Molecular cell*. 2020;80(4):633-47. e7.
52. Conklin KA. Chemotherapy-associated oxidative stress: impact on chemotherapeutic effectiveness. *Integrative cancer therapies*. 2004;3(4):294-300.
53. Marullo R, Werner E, Degtyareva N, Moore B, Altavilla G, Ramalingam SS, et al. Cisplatin induces a mitochondrial-ROS response that contributes to cytotoxicity depending on mitochondrial redox status and bioenergetic functions. *PLoS one*. 2013;8(11):e81162.
54. Choi Y-M, Kim H-K, Shim W, Anwar MA, Kwon J-W, Kwon H-K, et al. Mechanism of cisplatin-induced cytotoxicity is correlated to impaired metabolism due to mitochondrial ROS generation. *PLoS one*. 2015;10(8):e0135083.
55. Brozovic A, Ambriović-Ristov A, and Osmak M. The relationship between cisplatin-induced reactive oxygen species, glutathione, and BCL-2 and resistance to cisplatin. *Critical reviews in toxicology*. 2010;40(4):347-59.
56. He PJ, Ge RF, Mao WJ, Chung PS, Ahn JC, and Wu HT. Oxidative stress induced by carboplatin promotes apoptosis and inhibits migration of HN-3 cells. *Oncology letters*. 2018;16(6):7131-8.
57. Husain K, Whitworth C, Hazelrigg S, and Rybak L. Carboplatin-induced oxidative injury in rat inferior colliculus. *International journal of toxicology*. 2003;22(5):335-42.
58. Park M, Kim M, Suh Y, Kim R, Kim H, Lim E, et al. Novel signaling axis for ROS generation during K-Ras-induced cellular transformation. *Cell Death & Differentiation*. 2014;21(8):1185-97.
59. Weinberg F, Hamanaka R, Wheaton WW, Weinberg S, Joseph J, Lopez M, et al. Mitochondrial metabolism and ROS generation are essential for Kras-mediated tumorigenicity. *Proceedings of the National Academy of Sciences*. 2010;107(19):8788-93.
60. Schulze CJ, Seamon KJ, Zhao Y, Yang YC, Cregg J, Kim D, et al. Chemical remodeling of a cellular chaperone to target the active state of mutant KRAS. *Science*. 2023;381(6659):794-9.
61. Karachaliou N, Mayo C, Costa C, Magrí I, Gimenez-Capitan A, Molina-Vila MA, et al. KRAS mutations in lung cancer. *Clinical lung cancer*. 2013;14(3):205-14.
62. Do K, Speranza G, Bishop R, Khin S, Rubinstein L, Kinders RJ, et al. Biomarker-driven phase 2 study of MK-2206 and selumetinib (AZD6244, ARRY-142886) in patients with colorectal cancer. *Investigational new drugs*. 2015;33:720-8.
63. Jänne PA, van den Heuvel MM, Barlesi F, Cobo M, Mazieres J, Crinò L, et al. Selumetinib plus docetaxel compared with docetaxel alone and progression-free survival in patients with KRAS-mutant advanced non-small cell lung cancer: the SELECT-1 randomized clinical trial. *Jama*. 2017;317(18):1844-53.
64. Reck M, Carbone D, Garassino M, and Barlesi F. Targeting KRAS in non-small-cell lung cancer: recent progress and new approaches. *Annals of Oncology*. 2021;32(9):1101-10.
65. Yu F, Shi G, Cheng S, Chen J, Wu S-Y, Wang Z, et al. SUMO suppresses and MYC amplifies transcription globally by regulating CDK9 sumoylation. *Cell research*. 2018:1.
66. Dominissini D, Moshitch-Moshkovitz S, Schwartz S, Salmon-Divon M, Ungar L, Osenberg S, et al. Topology of the human and mouse m6A RNA methylomes revealed by m6A-seq. *Nature*. 2012;485(7397):201.
67. Ewels PA, Peltzer A, Fillinger S, Patel H, Alneberg J, Wilm A, et al. The nf-core framework for

- community-curated bioinformatics pipelines. *Nature biotechnology*. 2020;38(3):276-8.
68. Love MI, Huber W, and Anders S. Moderated estimation of fold change and dispersion for RNA-seq data with DESeq2. *Genome biology*. 2014;15:1-21.
 69. Yu G, Wang L-G, Han Y, and He Q-Y. clusterProfiler: an R package for comparing biological themes among gene clusters. *Omics: a journal of integrative biology*. 2012;16(5):284-7.
 70. Kanehisa M, and Goto S. KEGG: kyoto encyclopedia of genes and genomes. *Nucleic acids research*. 2000;28(1):27-30.
 71. Fabregat A, Jupe S, Matthews L, Sidiropoulos K, Gillespie M, Garapati P, et al. The reactome pathway knowledgebase. *Nucleic acids research*. 2018;46(D1):D649-D55.
 72. Benjamini Y, and Hochberg Y. Controlling the false discovery rate: a practical and powerful approach to multiple testing. *Journal of the Royal statistical society: series B (Methodological)*. 1995;57(1):289-300.
 73. Kim D, Paggi JM, Park C, Bennett C, and Salzberg SL. Graph-based genome alignment and genotyping with HISAT2 and HISAT-genotype. *Nature biotechnology*. 2019;37(8):907-15.
 74. Zhang Y, Liu T, Meyer CA, Eeckhoute J, Johnson DS, Bernstein BE, et al. Model-based analysis of ChIP-Seq (MACS). *Genome biology*. 2008;9:1-9.
 75. Ross-Innes CS, Stark R, Teschendorff AE, Holmes KA, Ali HR, Dunning MJ, et al. Differential oestrogen receptor binding is associated with clinical outcome in breast cancer. *Nature*. 2012;481(7381):389-93.
 76. Cui X, Wei Z, Zhang L, Liu H, Sun L, Zhang S-W, et al. Guitar: an R/bioconductor package for gene annotation guided transcriptomic analysis of RNA - related genomic features. *BioMed research international*. 2016;2016(1):8367534.
 77. Heinz S, Benner C, Spann N, Bertolino E, Lin YC, Laslo P, et al. Simple combinations of lineage-determining transcription factors prime cis-regulatory elements required for macrophage and B cell identities. *Molecular cell*. 2010;38(4):576-89.

Figure.1

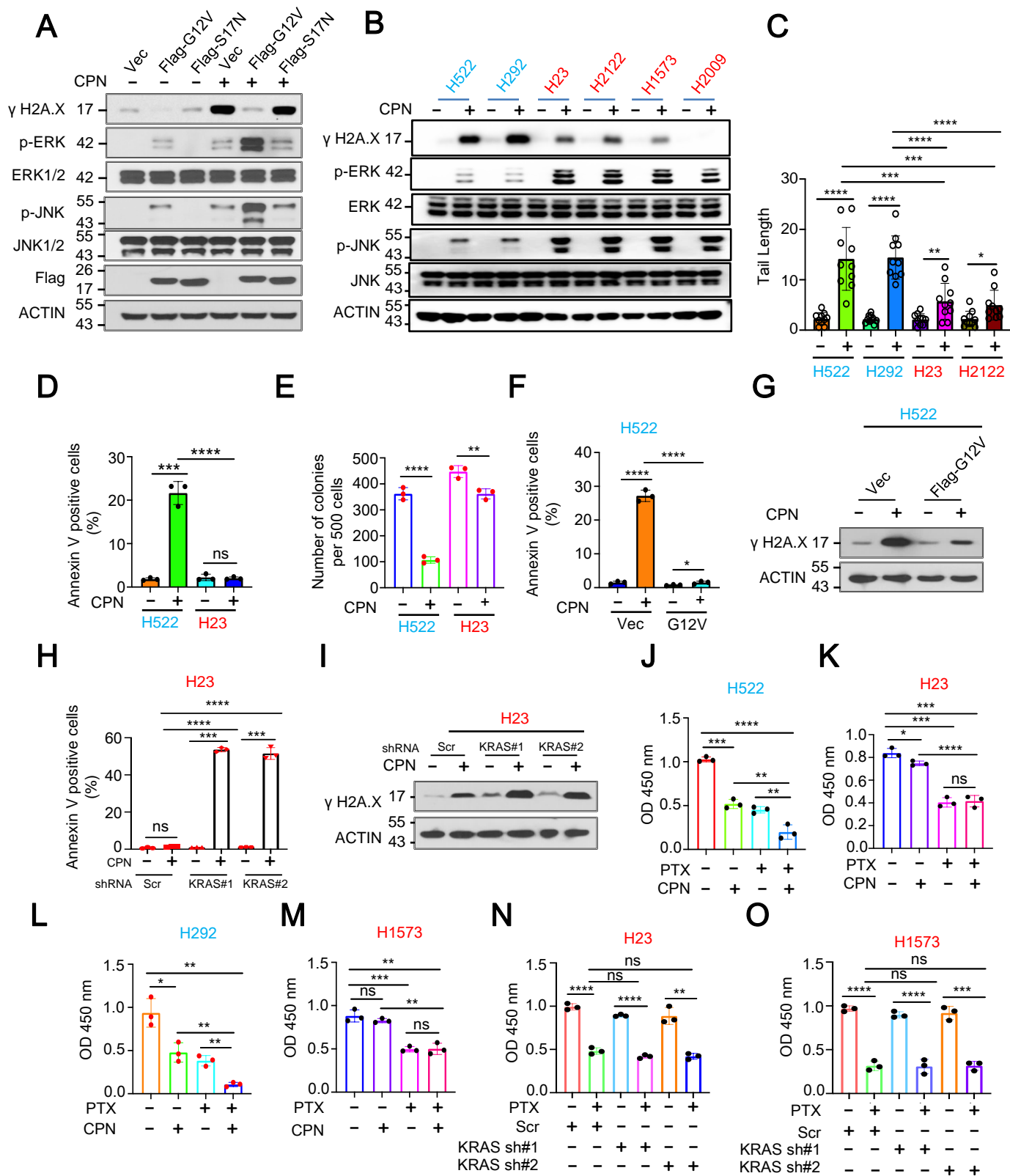


Figure.2

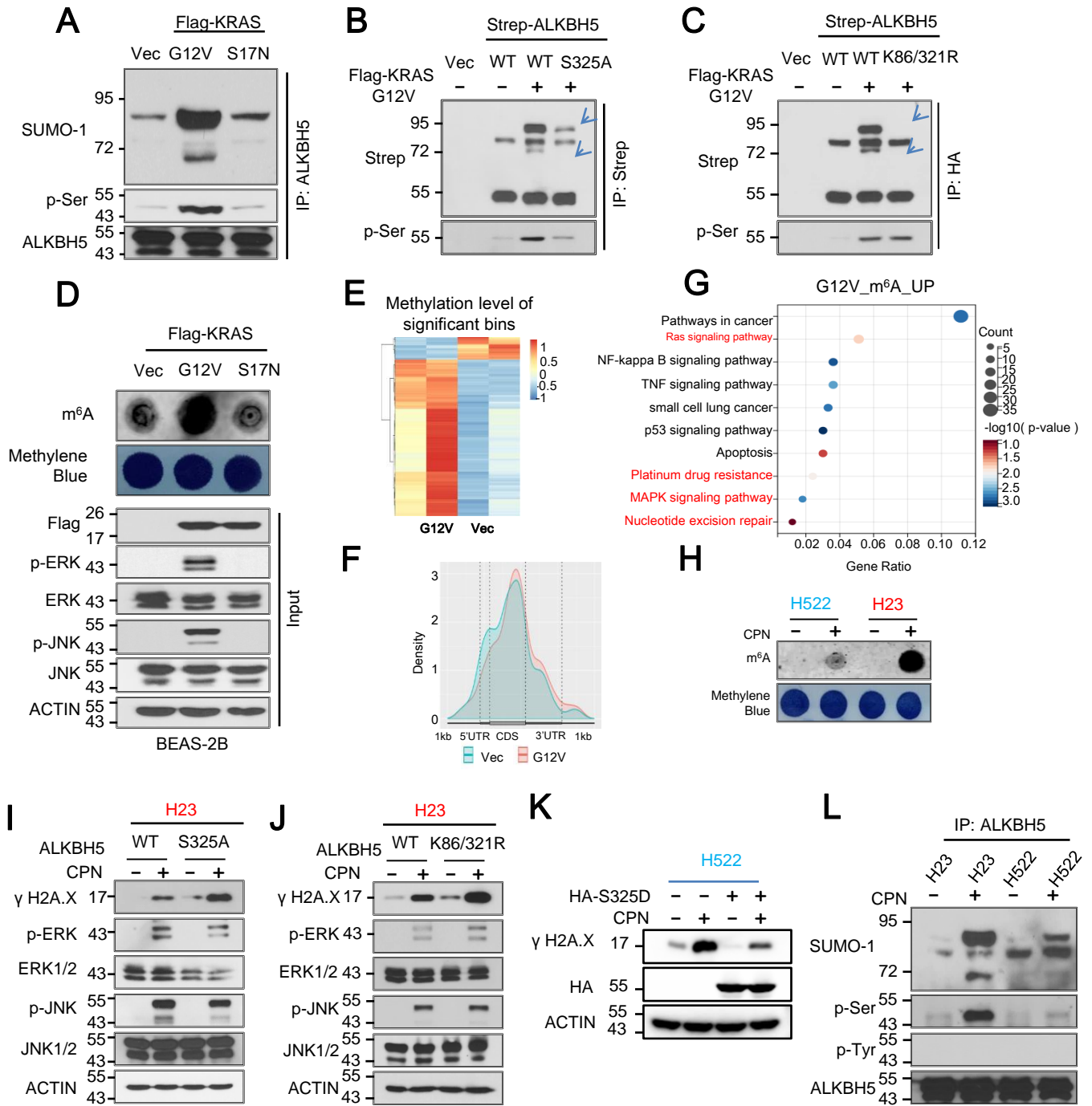


Figure.3

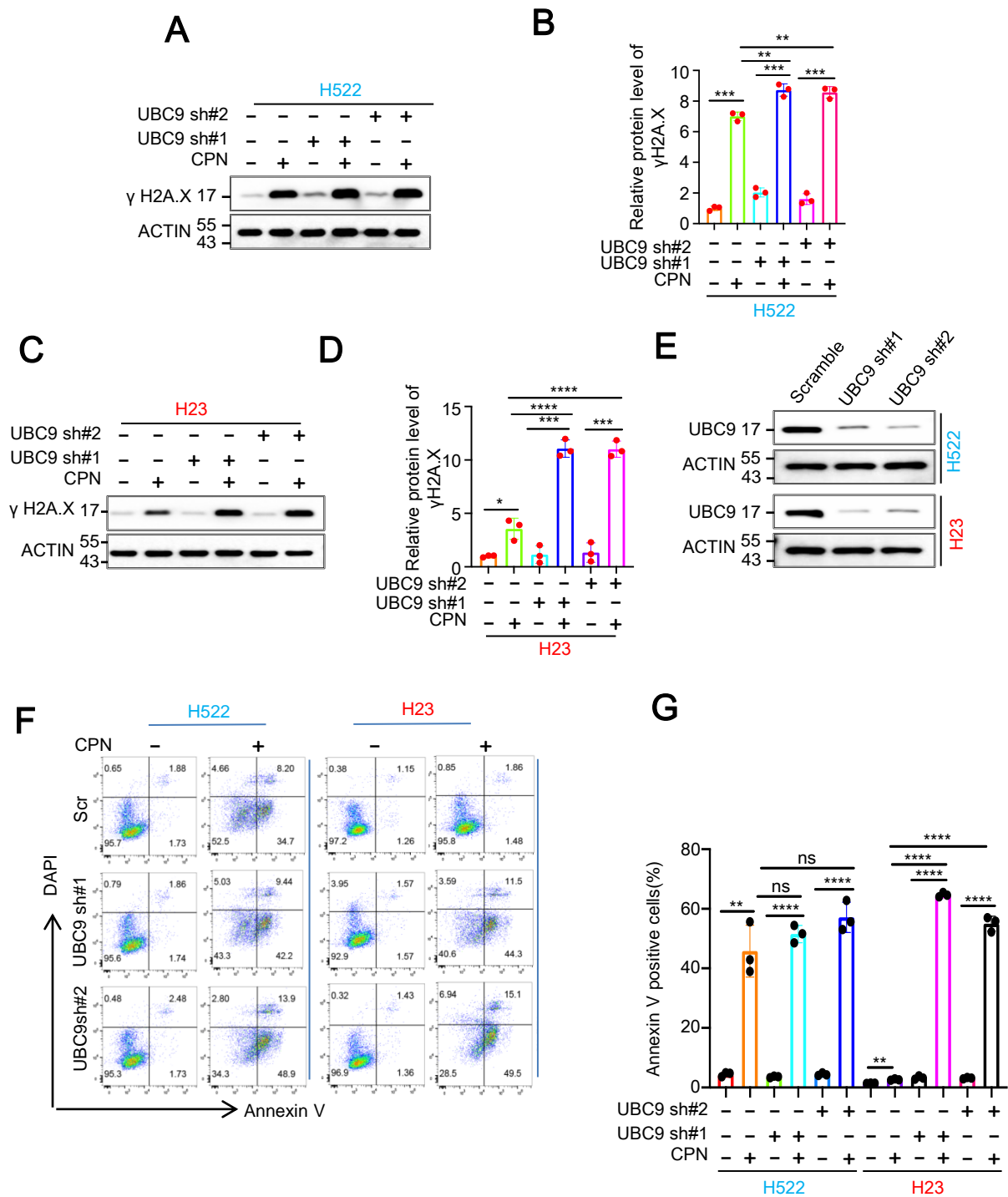


Figure.4

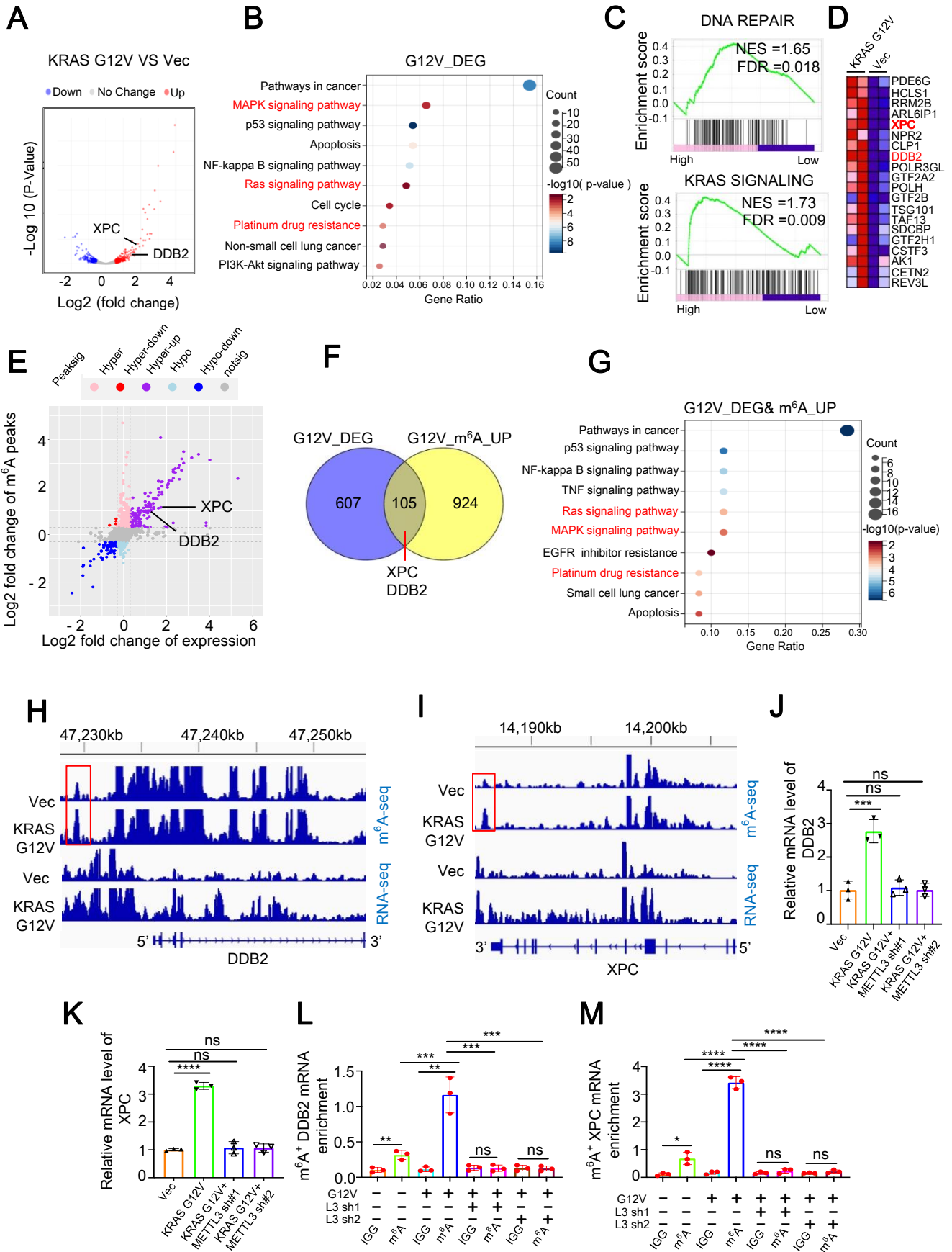


Figure.5

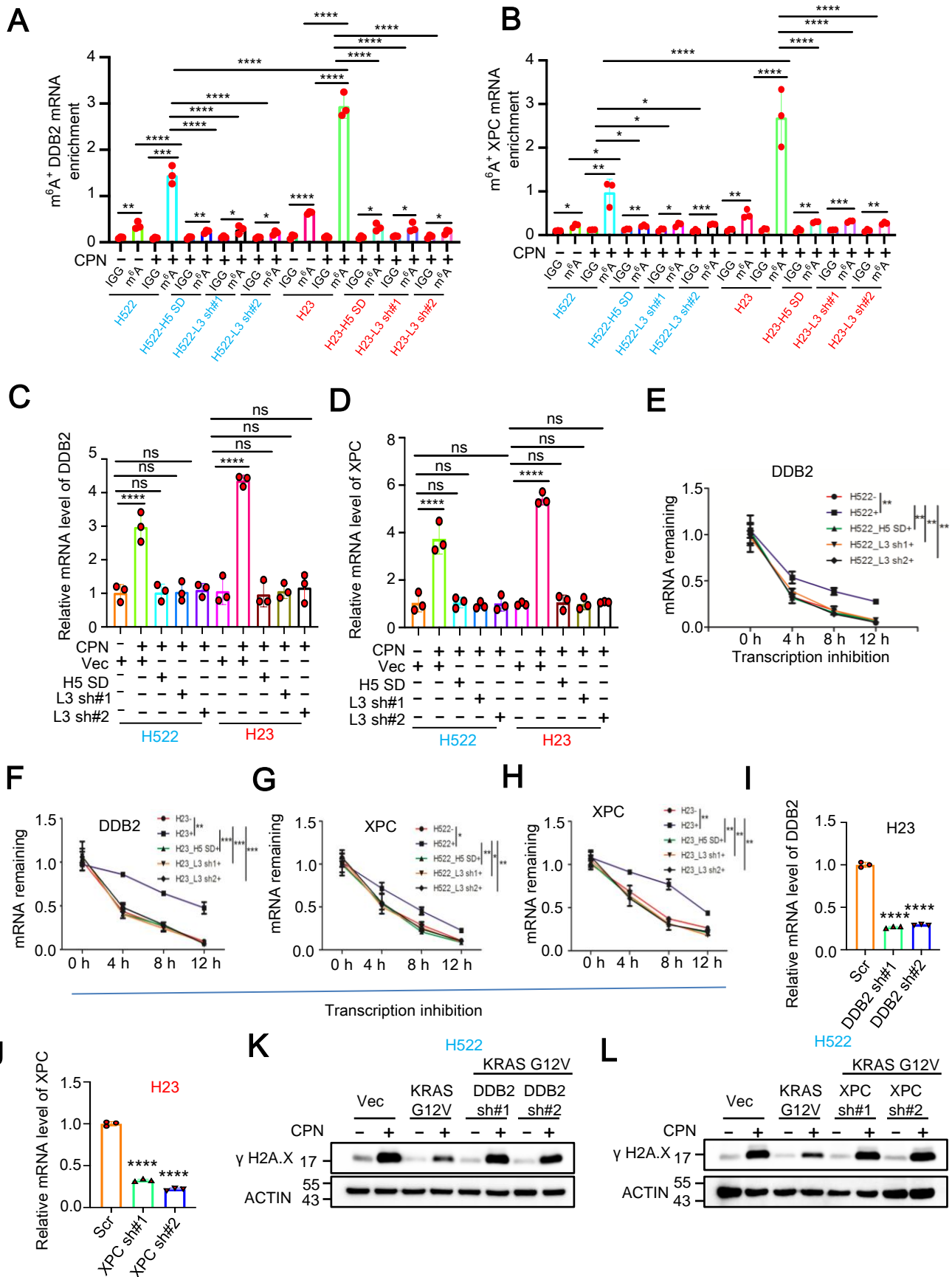


Figure.6

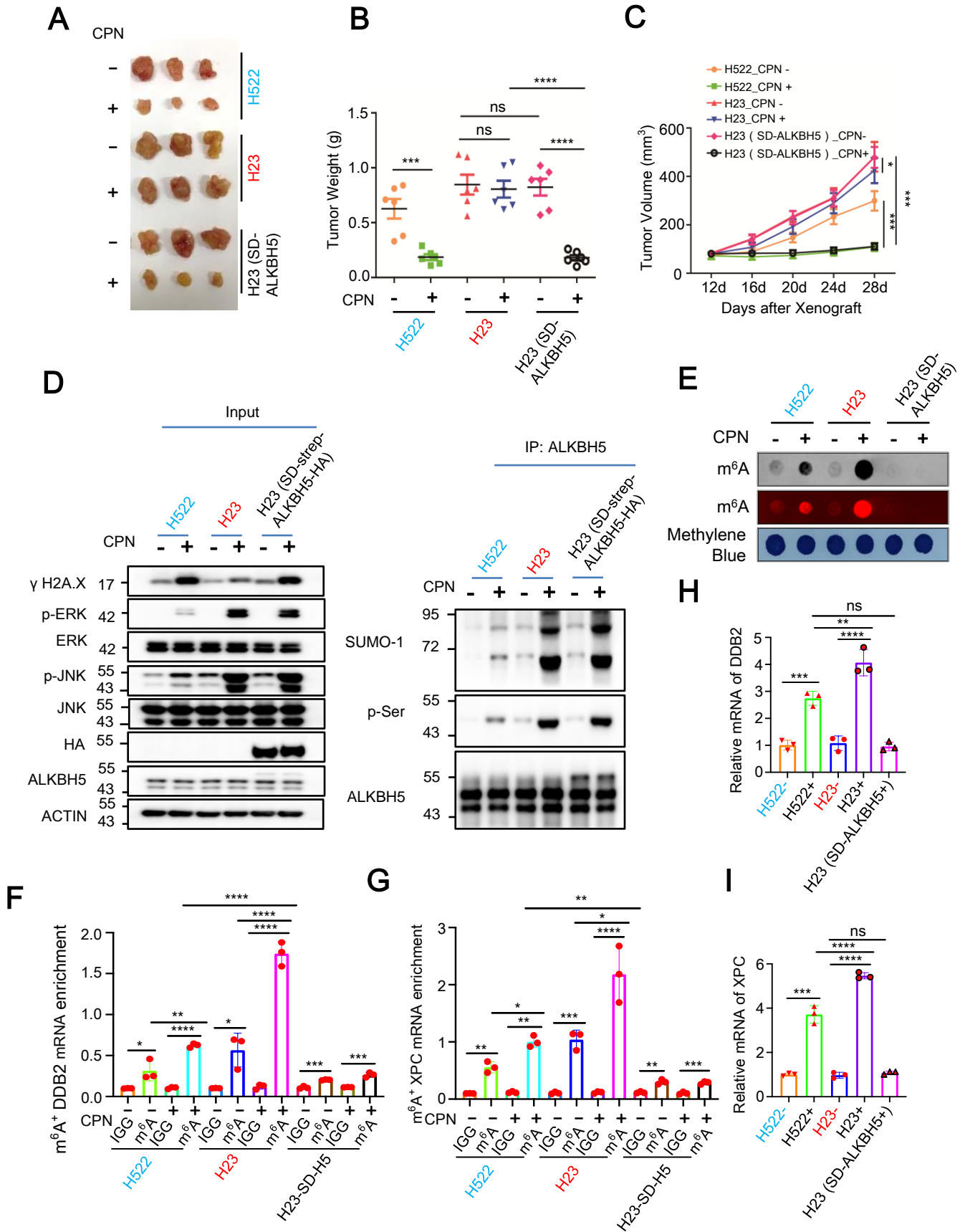


Figure.7

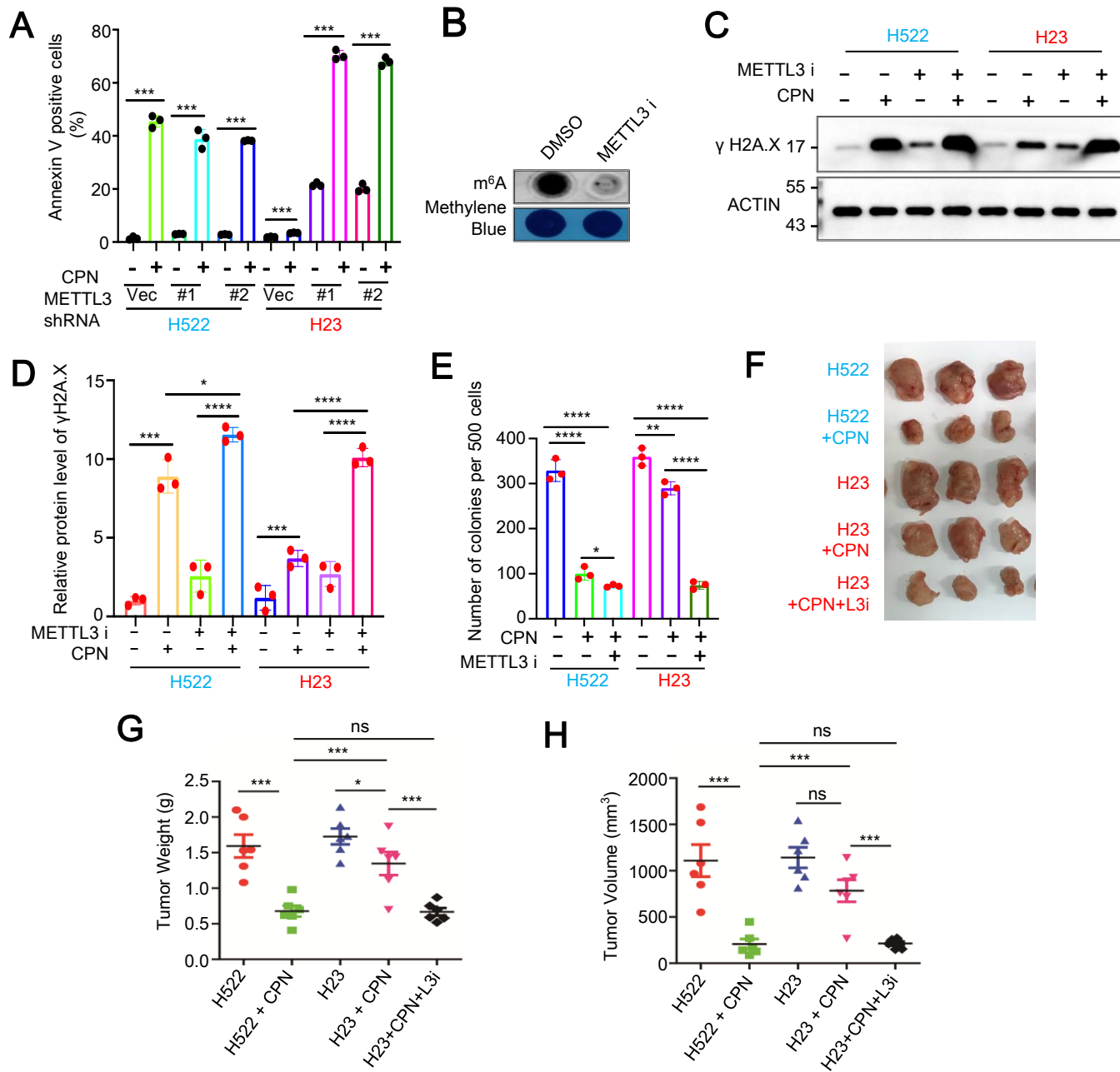


Figure.8

